

**G. Kotliar**  
Serin Physics Laboratory  
Rutgers University, Piscataway, NJ 08854

---

# The Mean Field Theory of the Mott Hubbard Transition

---

We describe the mean field theory of strongly correlated electrons which becomes exact in the limit of large lattice coordination and apply it to the Mott transition in the Hubbard model. We compare the predictions of the mean field theory with earlier approaches and with experiments on three dimensional transition metal oxides, and outline possible extensions of the approach.

---

## 1. SCOPE OF THIS ARTICLE

Recent experiments on heavy fermion systems, the high temperature superconductors and transition metal oxides, have revived the interest in strongly correlated electron systems. These are Fermi systems where the strength of the electron electron interactions is comparable to the kinetic energy. While the investigation of this class of systems goes back to the early sixties, so far a systematic tool to approach the problem has been lacking.

The essential physics lies in the interplay of the localization and the itineracy of the fermions, an effect that cannot be captured by the standard perturbative techniques. Recently a new mean field of the strong correlation problem was constructed.<sup>3,4,5</sup>

It is similar in spirit to the Weiss mean field theory in classical statistical mechanics. The technique is general and flexible and can be used to study a large class of lattice Fermi systems. This approach was motivated by the need to solve the quantum many body problem in the limit of infinite dimensions<sup>2</sup> but has already been applied to realistic three dimensional transition metal oxide systems.<sup>18</sup>

The essential idea is to replace the quantum many body problem by a single site problem in an effective medium which is solved for self consistently. The quantum mechanical nature of the problem is revealed in the complexity of the single site problem, which turns out to be an impurity model, with retarded interactions.<sup>3,10</sup> This self consistent zero dimensional problem can be attacked with a variety of techniques.

This approach should play the same role that mean field theory plays in classical statistical mechanics. It provides a simplified, but reliable picture of the various possible phases of a complex system and is a necessary first step in attacking complicated problems.

As in statistical mechanics the mean field theory becomes exact in the limit of large coordination, an aspect which ensures the internal consistency of the technique. This approach has already given new insights into problems such as the metal insulator transition in disordered systems<sup>51,52</sup> the superconductivity of strongly correlated electron systems<sup>11,12</sup> and the breakdown of fermi liquid theory in strongly correlated electron systems.<sup>6,7,8</sup>

In this article we will illustrate the use of the mean field technique using the Mott transition problem as an example. This article is not meant to be a review of the field of correlated electrons in the limit of large dimensions, a rapidly developing field with many active workers. For a more comprehensive review in that area the reader can turn to existing reviews in the literature.<sup>1</sup> Results on the Mott transition in large dimensions have appeared in Refs. 3, 10, 13, 23, 14, 15, 16, 17, 47, 42, 18.

In Section 2 we derive in detail the mean field theory of the paramagnetic phase of the Hubbard model. We follow the derivation of the Weiss mean field in the classical statistical mechanics of Ising systems and stress the analogies and the differences with the classical construction. The mean field theory forms a closed system of functional equations whose solution give all the local correlation functions of the lattice.

Before plunging into the analysis of these equations, we present some of the early concepts used to describe the interaction driven metal to insulator transition in Section 3.

In Section 4 we begin the analysis of the mean field equations and present some of the methods which resulted in useful insights. The quantum many body problem in the limit of large spatial coordination is an ideal testing ground for numerical and analytical techniques of quantum many body physics.

Section 5 describes the phase diagram of the half full Hubbard model. It exhibits a line of first order phase transitions joining a zero temperature critical point (the Mott transition point) and a finite temperature second order critical point. We

then illustrate the application of the mean field method at finite temperatures in the strong correlation region.

Section 6 is devoted to a discussion of the behavior of the physical quantities near the Mott point, comparing the field results with earlier studies of the Mott transition.

In Section 7 we compare predictions of the mean field theory with some experimental results on transition metal oxides.

We conclude with a brief discussion of the possible extensions of the method.

---

## 2. THE MEAN FIELD THEORY OF STRONGLY CORRELATED SYSTEMS

### 2.1 The Classical Analogy

The goal of a mean field theory is to reduce a many body, many site problem into a single site problem described by a mean field hamiltonian. For the ferromagnetic Ising model

$$H = \sum_{(ij)} J_{ij} S_i S_j + \sum_i h_i S_i \quad (1)$$

this is done by carrying out a partial trace over all the spin variables except for the spin at site  $o$  in the partition function

$$\frac{\int \prod_{i \neq 0} dS_i e^{-\beta H}}{\int \prod_i dS_i e^{-\beta H}} \equiv e^{-H_{eff}[S_0]} \quad (2)$$

$H_{eff}$  is the mean field hamiltonian in this problem in which one has replaced all the other spins by an effective field  $h_{eff}$ , the Weiss field .

$$H_{eff} = h_{eff} S_0 \quad (3)$$

We stress that knowledge of the mean field hamiltonian allows the calculation of all the *local* correlation functions of the original *lattice* problem.

So far this treatment is valid for an arbitrary lattice and in arbitrary number of dimensions. To obtain a mean field theory one has to relate  $h_{eff}$  to a local correlation function of the spins which in turn will be computed using the mean field Hamiltonian:

$$\begin{aligned} m &= \tanh \beta h_{eff} , \\ h_{eff} &= h + Jm . \end{aligned} \quad (4)$$

The last statement becomes exact in the limit of infinite dimensions provided that  $J_{ij}$  is scaled as  $J/2d$ . This statement is proved in the Appendix. This equation can of course be derived on physical grounds by replacing in Eq. (1)  $S_i$  by  $m$  to derive Eq. (3) and noticing that  $m$  computed with Eq. (3) is the local magnetization of the problem.

We presented the detailed derivation of this classic result because as we shall see in the following, it can be extended in a straightforward manner to quantum systems.

The starting point is the Hubbard model defined on an arbitrary lattice with hopping matrix elements  $t_{ij}$

$$H = - \sum_{ij} t_{ij} C_{i\sigma}^+ C_{j\sigma} + \mu \sum_i C_{i\sigma}^+ C_{i\sigma} + \sum_i U n_{i\uparrow} n_{i\downarrow} \quad (5)$$

with  $n_{i\sigma} \equiv C_{i\sigma}^+ C_{i\sigma}$ .

For this model one writes the partition function (and the corresponding correlation function) as functional averages over Grassman variables with weight  $L$ ,

$$Z = \int \prod_i dC_{i\sigma}^+ dC_{i\sigma} e^{-L}, \quad (6)$$

$$L = \int_0^\beta (d\tau \sum_i C_{i\sigma}^+ \frac{\partial}{\partial \tau} C_{i\sigma} - \sum_{(ij)} t_{ij} C_{i\sigma}^+ C_{j\sigma} + \mu \sum_i C_{i\sigma}^+ C_{i\sigma}) + U \sum_i \int_0^\beta d\tau n_{i\uparrow} n_{i\downarrow}. \quad (7)$$

We follow closely the Ising analogy. We first trace out all the spins except for site  $o$ , to get an effective action for the degrees of freedom located at the origin,

$$e^{-S_{eff}[C_o^+ C_o]} \equiv \frac{\int \prod_{i \neq o} dC_i^+ dC_i e^{-L}}{\int \prod_i dC_i^+ dC_i e^{-L}}. \quad (8)$$

$S_{eff}$  in the paramagnetic phase has the form

$$S_{eff}(\Gamma) = \sum_{n=1}^{\infty} \int d\tau_i ds_j \Gamma^{\alpha_1 \dots \alpha_n \beta_1 \dots \beta_n} [\tau_1 \dots \tau_n s_1 \dots s_n] C_{\alpha_1}^+(\tau_1) \dots C_{\alpha_n}^+(\tau_n) C_{\beta_1}(s_1) \dots C_{\beta_n}(s_n) \quad (9)$$

where we have dropped the subscript zero on the site orbital. The functions  $\Gamma^{\alpha_1 \dots \beta_n} [\tau_1 \dots s_n]$  containing the effects of the medium are discussed in Appendix 2.

Notice that the knowledge of  $S_{eff}$  allows us to calculate *all the local* correlation functions of the original Hubbard model. This observation is valid in any number of dimensions. To obtain a mean field theory one has to connect the coefficients of the effective action to local correlation functions which can be computed using  $S_{eff}$ . It turns out that this step can be carried out exactly in two cases: a) on the Bethe

lattice with finite branching ratio<sup>51</sup> b) on lattices with more general connectivity provided that the matrix elements  $t_{i,j}$  fall off as  $\frac{1}{\sqrt{d}^{|i-j|}}$  and the limit of large  $d$  is taken. This is the limit of infinite dimensions or infinite spatial connectivity which was introduced by Metzner and Vollhardt.<sup>2</sup>

The equations obtained in both cases are different and so far only the second set of mean field equations has been thoroughly explored. The explicit form of the functional  $S_{eff}$  is derived in Appendix 2. Here we summarize the results in the limit of large lattice coordination. The effective action has a simple form:

$$S_{eff}[G_0] = \int_0^\beta \int_0^\beta C_\sigma^+ [-G_0^{-1}] C_\sigma + \int_0^\beta U C_\uparrow^+ C_\uparrow C_\downarrow^+ C_\downarrow . \quad (10)$$

The function  $G_0(\tau - \tau')$  will play the role of the Weiss field of the problem. As in any mean field theory the Weiss field can be expressed in terms of a local quantity, in this case local Greens function of the problem. The self consistency condition derived in Appendix 2 is the algebraic relation:

$$G_0^{-1}(i\omega_r) = \frac{1}{G(i\omega_r)} - \Phi^{-1}(G(i\omega_r)) + \mu + i\omega_r \quad (11)$$

$\Phi$  is the Hilbert transform of the lattice density of states,  $\Phi(Z) \equiv \int d\epsilon \rho(\epsilon)/(Z - \epsilon)$ .

Since the local Greens function  $G(\tau - \tau')$  can be calculated using the effective action (10),

$$G(\tau - \tau') = \frac{\int dC^+ dC C^+(\tau') C(\tau) e^{-S_{eff}(G_0)}}{\int dC^+ dC e^{-S_{eff}(G_0)}} . \quad (12)$$

The closed system of Eqs. (10), (11), and (12) is the mean field theory of strongly correlated electrons systems. It is exact in the limit of large lattice coordination. The simplicity of the theory is largely the results of the lack of renormalization of all the higher vertices. In this order the only quartic term in the action is the original local repulsion  $U$  of the Hubbard model.

To solve the mean field equations one begins with a guess for the Weiss field function  $G_0$ , which is then inserted in the effective action to compute the functional integral<sup>12</sup> which gives the one particle greens function of the Anderson impurity mode with a bath  $G_0$ . One then substitutes the local Greens function  $G$  into the self consistency Eqs. (11) to obtain the next guess for  $G_0$ . This procedure, (known as substitution iteration), is continued until it converges and is illustrated in Fig. 1. Near a phase transition the standard improvements for solving non linear systems of equations, such as the Newton Rawsen method, are necessary to improve the rate of convergence.

Notice that as in the context of the Ising model one can guess these equations using simple physical arguments. The local description of the physics at site 0 is to be provided by an impurity action of the form (10). This impurity action can be used to calculate the local impurity Green's function and the impurity self energy as a functional of  $G_0$ ,  $G_{imp}\{G_0\}(i\omega_r)$ ,  $\Sigma_{imp}\{G_0\} \equiv G_{imp}^{-1}\{G_0\}(i\omega_r) - G_0^{-1}(i\omega_r)$ .

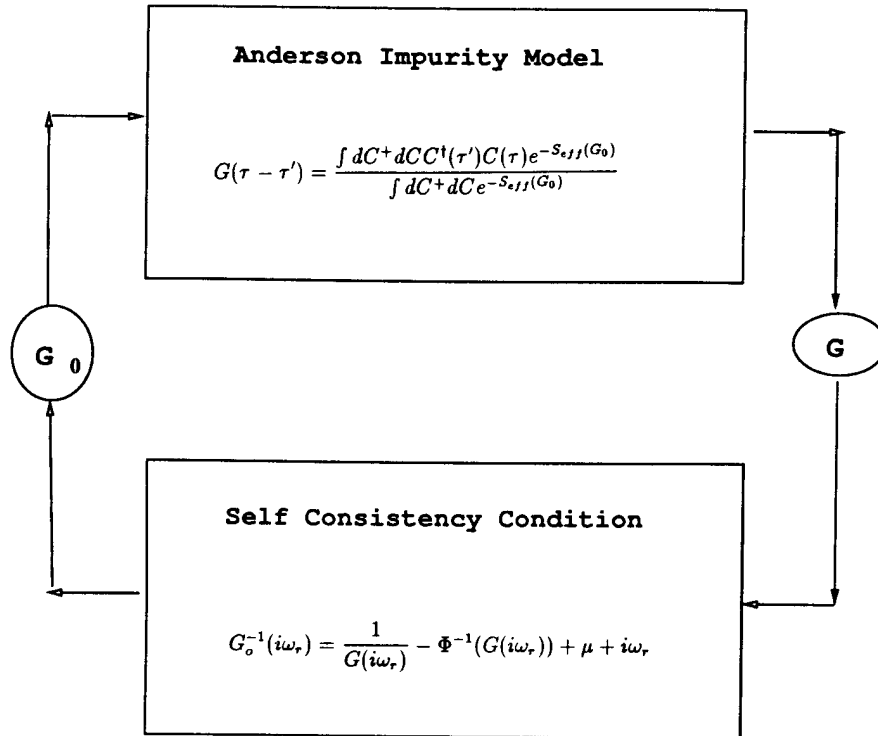


**FIGURE 1.** Schematic representation of the self consistent equations for the Green's functions and the Weiss field.

Requiring that the impurity self energy and the Green's function self energy are indeed the local Green's function and the self energy of the original Hubbard model gives the self consistency equation,

$$(G_0^{-1} - \Sigma_{imp}\{G_0\})^{-1} = \int \frac{\rho(\epsilon)}{i\omega_r - \epsilon + \mu - \Sigma_{imp}\{G_0\}}. \quad (13)$$

Eq. (13) is completely equivalent to the self consistency condition Eq. (11). Notice that  $\rho(\epsilon) = \sum_k \delta(\epsilon - \epsilon_k)$ ,  $\epsilon_k = \sum_j t_{ij} e^{ik(\tau_i - \tau_j)}$  is the only place where the precise form of the lattice enters the mean field equations. In the spirit of mean field theory, one should use the mean field equations to calculate local properties of realistic lattices by inserting in Eqs. (13) or (11) the appropriate density of states.

## 2.1 Physical content of the mean field theory

The structure of the mean field theory is that of a functional equation for the Weiss field  $G_0$  and the local Green's function  $G$ . The physical interpretation of the "mean field action" is obtained by noticing that the path integral in Eqs. (10), and (12) describes an Anderson impurity model. This model consists of four local states ( $|0\rangle, |\uparrow\rangle, |\downarrow\rangle, |\uparrow, \downarrow\rangle$ ) embedded in a medium described by the "conduction electrons" operators  $a_k$ ,

$$H_{AM} = \sum_k \epsilon_k a_{k\sigma}^+ a_{k\sigma} + U f_{\uparrow}^+ f_{\uparrow} f_{\downarrow}^+ f_{\downarrow} + \sum_k V_k (a_{k\sigma}^+ f_{\sigma} + f_{\sigma}^+ a_{k\sigma}) + \epsilon_f f_{\sigma}^+ f_{\sigma} . \quad (14)$$

Integrating out the electrons  $a_{k\sigma}^+ a_{k\sigma}$  in a functional integral formulation of the Anderson impurity model gives rise to an action of the form Eq. (10) with,

$$G_0^{-1} = i\omega_r - \epsilon_f - \Delta(i\omega_r) , \quad \Delta(i\omega_r) = \sum_k \frac{V_k^2}{(i\omega_r - \epsilon_k)} , \quad (15)$$

therefore it is clear that Eq. (10) describes a quantum degree of freedom  $f_{\sigma}$  hybridizing with a bath of conduction electrons. The Weiss field  $G_0^{-1}$  describes the dynamics of that bath, and  $\epsilon_f$  should be identified with the minus the chemical potential of the large  $d$  Hubbard model.

Eqs. (10), (11), and (12) are the the natural formulation of mean-field theory for quantum models.<sup>3</sup> Due to the freezing of spatial fluctuations, one-particle properties can be understood by looking at a single fixed site of the lattice. Because the model is itinerant, the occupation of this site undergoes quantum fluctuations (in imaginary time) between empty, occupied by an "up" or a "down" spin, and doubly occupied. The quantum dynamics of these processes is described by  $S_{imp}$ , where  $G_0$  is an *effective* quantity determined by all the processes happening on the other sites.  $G_0$  should be thought of as the appropriate generalization to quantum itinerant systems of the effective field in the familiar mean-field theory of a classical spin system. The correspondence between the classical and the quantum mean field construction is illustrated in Table 1.

The necessity to have a function which plays the role of effective field is dictated by an important aspect of the physics of strongly correlated electrons: the presence of several *energy scales* in this problem (even infinitely many in phases exhibiting self similar correlation functions<sup>6</sup>). This information cannot be stored using a single number and we must use a function containing the various energy scales and their relative spectral weight to play the role of the effective field of the mean field theory. A similar situation arises in the mean field theory of spin glasses.

Table 1

Quantum Case	Classical Case	
$\sum_{(ij)} t_{ij} C_{i\sigma}^+ C_{j\sigma} + U \sum_i n_{i\uparrow} n_{i\downarrow}$	$H = \sum_{(ij)} J_{ij} S_i S_j + r_i S_i$	Hamiltonian
$t_{ij} \sim \left(\frac{1}{\sqrt{d}}\right)^{ i-j }$	$J_{ij} \sim \left(\frac{1}{d}\right)^{ i-j }$ (ferromagnet)	Scaling
$G(k, i\omega_r) = \langle C_K^+(i\omega_r) C_K(i\omega_r) \rangle$	$\langle S_i S_j \rangle$	Correlation Function
$\langle C^+(i\omega_r) C(i\omega_r) \rangle$	$m = \langle S_i \rangle$	Local Observable
$\int \int C_\sigma^+(\tau) - G_0^{-1}(\tau - \tau') C_\sigma(\tau') + \int U n_\uparrow n_\downarrow$	$H_{eff} = h_{eff} S_o$	Single Site Hamiltonian
$H = \sum_K A_{K\sigma}^+ A_{K\sigma} \epsilon_K + \sum_K V_K C_\sigma^+ A_{K\sigma}$		
$+ U n_\uparrow n_\downarrow$		
$G_o^{-1}(i\omega_r)$	$h_{eff}$	Weiss Field
$G_o^{-1}(i\omega_r) = G^{-1}(i\omega_r) - \Phi^{-1}[G(i\omega_r)] + \mu + i\omega_r$	$h_{eff} = \frac{1}{2} \arctan[m]$	Relation between Weiss Field and Local Observable

Earlier approaches which are sometimes labeled as mean field theories, like Hartree Fock, RPA, slave boson large N, can be viewed in this light as a parametrization of the function  $G$  by means of a single number whose physical meaning is usually related to the *lowest energy scale* of the problem.

### 2.3 Connection with the limit of large lattice coordination

We have shown that when the hopping matrix elements are suitably scaled, all the local observables can be computed from the closed set of mean field equations. This is the limit of infinite dimensionality introduced by Metzner and Vollhardt.<sup>2</sup> In this limit the knowledge of the local correlation functions allows us to reconstruct uniquely all the  $k$  dependent lattice correlation functions. The natural strategy for calculating all the  $n$ -point functions of the Hubbard model in the limit of large coordination is therefore to compute the local correlators in the impurity model and to reconstruct the  $k$  dependence of the lattice correlation function by inserting the impurity quantities in the formulae below.

We illustrate this by the example of the one particle Green's function

$$G(k, i\omega_r) = - \langle C(k, i\omega_r) C^+(k, i\omega_r) \rangle = \frac{1}{i\omega_r + \mu - \epsilon_k - \Sigma(i\omega_r)} \quad (16)$$

where the self energy is  $k$  independent. Therefore the local Green's function is given by  $G_L(i\omega_r) = \Phi(Z) \equiv \int d\epsilon \rho(\epsilon)/(Z - \epsilon)$ ,  $\Phi$  is the Hilbert transform of the lattice density of states and  $Z = i\omega_r + \mu - \Sigma(i\omega_r)$ . Knowledge of  $G_L(i\omega_r)$  allows us to express  $G(K, i\omega_r)$  as

$$G(K, i\omega_r) = [\Phi^{-1}(G_L(i\omega_r)) - \epsilon_K]^{-1}. \quad (17)$$

The density of states determines all the local properties. Magnetic properties, such as the Néel temperature, on the other hand will depend on the nature of the lattice, (i.e. the degree of magnetic frustration). Notice there are many lattices in large dimensions, which give rise to the same density of states, and as a consequence, to the same local Greens function. This freedom will be crucial in our study of the Mott transition because it will allow us to vary the degree of magnetic frustration keeping the same local density of states. It is instructive to illustrate this point with various examples.

For a  $d$ -dimensional hypercubic lattice with  $t_{ij} = t/\sqrt{d}$  for nearest neighbors and zero otherwise, one has:

$$\rho(\epsilon) = \frac{1}{\sqrt{\pi t}} \exp(-\frac{\epsilon^2}{D^2}) \quad (18)$$

In this case  $D = t$ . The same density of states is obtained in the hypercubic lattice with next nearest neighbor hopping. In this case  $D = \sqrt{t_1^2 + t^2}$ . This lattice is magnetically frustrated.

The semicircular density of states is realized in the Bethe lattice with coordination  $d$ , in the limit that  $d$  becomes infinite, and with Hubbard's hopping parameter equal to  $\frac{t}{\sqrt{d}}$ . In this case  $t = D/2$ . This lattice is not frustrated, and orders antiferromagnetically at low temperatures,

$$\rho(\epsilon) = \frac{1}{\pi} \sqrt{\epsilon^2 - D^2} \quad |\epsilon| < D. \quad (19)$$

With this density of states the self consistency condition connecting the Greens function and the Weiss field is given by:

$$G_o^{-1} = i\omega_r + \mu - t^2 G(i\omega_r). \quad (20)$$

The semicircular density of states is also realized in the fully frustrated model.<sup>23,17</sup>

$$H_{FF} = -t \sum_{i,j=1,d} \epsilon_{ij} c_{i\sigma}^\dagger c_{j\sigma} + U \sum_i n_{i\uparrow} n_{i\downarrow} \quad (21)$$

Summation over repeated spin indices is assumed. Here  $\epsilon_{ij}$  are quenched independently distributed Gaussian random variables with zero mean and a variance  $\langle \epsilon_{ij}^2 \rangle = 1/d$ . This model has a semicircular density of states with a bandwidth equal to  $2t$  and therefore shares the same *local* properties as the Bethe lattice but of course is not expected to display Néel order at any finite temperature. Finally

we can vary the degree of frustration by studying a two sublattice version of the fully frustrated model (TSFFM). The Hamiltonian is given by:

$$H_{TSFFM} = -t_1 \sum_{i,j \in A \text{ or } B} \epsilon_{ij} c_{i\sigma}^\dagger c_{j\sigma} - t_2 \sum_{i \in A, j \in B} \epsilon_{ij} c_{i\sigma}^\dagger c_{j\sigma} + U \sum_{i \in A \cup B} n_{i\uparrow} n_{i\downarrow}. \quad (22)$$

This model interpolates between the fully frustrated lattice and the Bethe lattice in the antiferromagnetic phase while still sharing a semicircular local density of states. In this case  $D = \frac{\sqrt{t_1^2 + t_2^2}}{2}$ . Notice that while the hamiltonians Eqs. (21) and (22) contain randomness, the single particle properties are self averaging. The single particle Green's functions are the same for any typical realization of the random variables  $\epsilon_{ij}$ .

Both Eqs. (22) and (21) are toy models representing a frustrated lattice with a semicircular local density of states having well defined large  $d$  limits. The results obtained for these models are representatives of what one would obtain if the mean field theory was applied directly to realistic frustrated lattices.

## 2.4 Extension to Broken Symmetries

The mean field framework can be easily extended to incorporate magnetic long range order. Here we discuss the extension in the case of a bipartite structure with semicircular density of states such as the Bethe lattice or the two sublattice fully frustrated model. The original extension of the mean field framework was carried out in Ref. 10 while the extension to incorporate a superconducting order parameter appeared in Ref. 11.

When antiferromagnetism sets in, the cavity derivation of the mean field equations is still valid but one can no longer assume spin or translation invariance of the effective action. The Weiss field depends on the sublattice and the spin. In a general bipartite lattice in the Néel phase  $G_{A\sigma} = G_{B-\sigma}$  and the sublattice dependent effective action becomes:

$$S_{eff A,B}[G_{0A,B}] = \int_0^\beta \int_0^\beta C_\sigma^+ [-G_{0A,B}^{-1} \sigma] C_\sigma + \int_0^\beta U C_\uparrow^+ C_\uparrow C_\downarrow^+ C_\downarrow \quad (23)$$

For the Bethe lattice, the equations of Ref. 10. simplify to:

$$G_{0A\sigma}^{-1} = i\omega - t^2 G_{B\sigma}, \quad (24)$$

$$G_{0B\sigma}^{-1} = i\omega - t^2 G_{A\sigma}, \quad (25)$$

where  $A$  denotes one sublattice and  $B$  the other. The two impurity Green's functions  $G_A$  and  $G_B$  are evaluated independently given  $G_{0A\sigma}$  and  $G_{0B\sigma}$  using the single site action Eq. (23).

Finally in the two sublattice fully frustrated model (TSFFM), which mimics an intermediate degree of frustration, the mean field equations in a phase where the  $A$  and  $B$  sublattices magnetize in opposite directions are given by,

$$G_{0A\sigma}^{-1} = i\omega - t_1^2 G_{A\sigma} - t_2^2 G_{B\sigma} , \quad (26)$$

$$G_{0B\sigma}^{-1} = i\omega - t_1^2 G_{B\sigma} - t_2^2 G_{A\sigma} . \quad (27)$$

---

### 3. THE MOTT TRANSITION

The Mott transition, that is the metal insulator transition induced by the electron electron interactions in a periodic system, has been investigated theoretically and experimentally for many years.<sup>19</sup> Experimentally it is realized in three dimensional transition metal oxides such as  $V_2O_3$  and  $NiI_2$  and can be driven by varying pressure temperature and composition.

From a theoretical point of view, several ideas have been put forward. Hubbard first introduced the notion of Hubbard bands. These describe propagating empty and doubly occupied sites in a half full lattice. For large  $U$  these bands are separated by a gap of order  $U - 2D$ . As  $U$  is reduced there is a critical value of  $U$  where the two bands merge again.<sup>20</sup> This is the Hubbard picture of the metal insulation transition.

Brinkman and Rice,<sup>21</sup> building on the work of Gutzwiller, started from the metallic phase which they described as a strongly renormalized Fermi liquid with a characteristic Fermi energy scale. As the interaction strength increases this energy vanishes at a critical value of the interaction  $U$ . In this framework the metal insulator transition is driven by the disappearance of the Fermi liquid quasiparticles.

Slater<sup>22</sup> pointed out that the metal insulator transition is always accompanied by long range antiferromagnetic order, and viewed the doubling of the unit cell which makes the band structure of the system that of a band-insulator, as the driving force behind the metal insulator transition.

---

### 4. METHODOLOGY

The mean field equations are coupled functional equations to be solved for the Weiss field and the local Greens function. The most difficult aspect of the mean field theory is the solution of the Anderson impurity model in an arbitrary bath. This class of problems has been studied intensively in the last 40 years and we will draw on this knowledge to make exact and approximate statements on the solution of lattice models in large dimensions. The essential insight is to use *reliable*

approximations to calculate  $G\{G_0\}$  in Eq. (12), this step captures the local aspects of the problem. The self consistency condition Eq. (11) then brings back the lattice aspect of the problem.

Several techniques that have been used in the analysis of the mean field equations, they range from qualitative arguments and analytic perturbative schemes to numerical methods based on Quantum Montecarlo and exact diagonalization. All the insights obtained on the Mott transition problem rely on a combination of these techniques.

#### 4.1 Qualitative arguments

We begin the analysis of the mean field Eqs. (10), (11), and (12) at zero temperature.

**Small U limit.** In this limit the self energy of the Anderson impurity model is a smooth function of frequency that can be computed perturbatively in the interaction  $U$ . At half filling particle hole symmetry implies  $\lim_{\omega \rightarrow 0} \Sigma(i\omega) = 0$ . The self consistency condition then implies that as long as one is in the Fermi liquid phase the value of  $G(i\omega = 0) = 2/D$  is pinned independent of the interaction strength.<sup>9</sup> The self consistency condition Eq. (80) implies that  $\lim_{\omega \rightarrow 0} G_0^{-1}(i\omega) = iD/2$ . Since the latter is the low frequency limit of the hybridization function of the Anderson impurity model (Eq. (15)) we have a standard Anderson model describing an impurity embedded in a *regular* bath of conduction electrons with a *non singular density of states at the Fermi level*. The low frequency behavior of the self energy is given by  $\Sigma(i\omega) \approx (Z^{-1} - 1)i\omega$  which defines the renormalized Fermi energy of the problem  $ZD$ . A plot of the spectral function for various values of  $U$  is shown in Fig. 2. For very small  $U$ ,  $Z$  is close to one and the spectral function of the impurity is featureless and identical to the bare lattice density of states.

For intermediate values of  $U$ ,  $Z^{-1}$  is larger and we expect a feature at the Fermi level which corresponds to the Abrikosov Suhl resonance and two features at energies  $\pm U$  which correspond to the upper and lower Hubbard band of the large  $d$  Hubbard model or to the occupied and unoccupied atomic  $f$  level of the Anderson impurity model. Near the disappearance of the central peak in Fig. 2 a new small energy scale emerges, the renormalized Fermi energy  $\Delta D$ , where  $\Delta \approx Z^{-1}$  is the spectral weight at low energies.

**Large U limit.** When  $U$  is large we begin with a different ansatz. We expect  $G$  to be a superposition of two magnetic Hartree Fock solutions:

$$G_L(i\omega) = \frac{1/2}{G_0^{-1}(i\omega_n) - U/2} + \frac{1/2}{G_0^{-1}(i\omega_n) + U/2}. \quad (28)$$

This in turn implies that  $G(i\Omega) \approx i\Omega$  and the substitution into the self consistency condition implies that  $G_0^{-1} \approx i\Omega$  which in turn implies that the effective bath in the Anderson model picture *has a gap*.

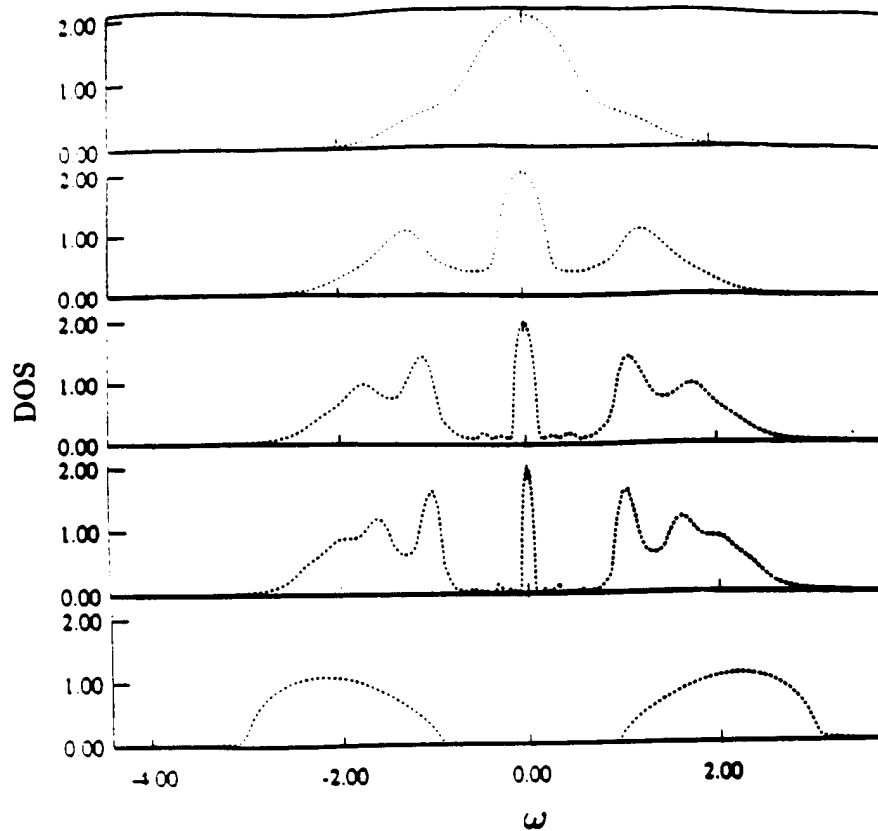


**FIGURE 2.** Schematic plot of the conduction electrons states and the impurity configurations, illustrating the low and high energy parts near  $U_{c2}$ .

We can now check that the Ansatz we made is self consistent because we know from the theory of an Anderson impurity embedded in a *semiconducting medium* that the Kondo effect does not take place, showing that the superposition of two magnetic Hartree Fock solutions is a self consistent Ansatz.<sup>23</sup>

**Existence of a Mott transition.** We have established analytically the existence, at zero temperature, of two classes of solutions. a) metallic, characterized by a non zero density of states of the impurity and the bath. b) insulating, characterized by zero density of states of the impurity and the bath of conduction electrons at zero frequency.

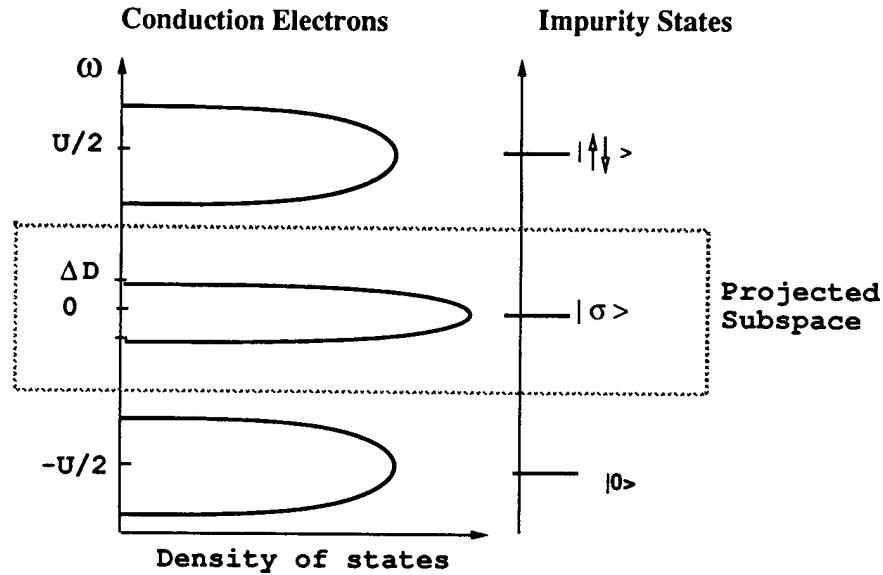


**FIGURE 3.** One particle spectral functions for various values of the interaction  $U = 1, 2, 2.7, 3, 4$ . obtained from the second order perturbation approach.

The density of states at zero energy is like an order parameter for this problem and one cannot go from a) to b) without undergoing a phase transition at a critical value  $U$ . We have established *analytically* the existence of a Mott transition in the paramagnetic phase of the large  $d$  Hubbard model at zero temperature.<sup>23,13</sup> The evolution of the one particle spectral function as a function of  $U$  is sketched in Fig. 3.

#### 4.2 Quantum Monte Carlo

Numerical schemes introduce a *discrete* parametrization of the Greens functions, and the Weiss field, involving a finite number  $N_p$  of parameters and reduce the system of functional Eqs. (10), (11), and (12) to a system of  $N_p$  non linear equations in  $N_p$  unknowns. The hope is that as  $N_p$  increases physical quantities converge relatively fast to their physical values so that this converged value can be inferred by extrapolating results obtained from a finite (and usually small) number of parameters  $N_p$ . The application of Quantum Monte Carlo methods to impurity models was carried out by Hirsch and Fye.<sup>26</sup> Here we present an alternative derivation of this class of algorithms.

To apply the quantum Monte Carlo method to our problem one parametrizes  $G(\tau)$  in  $[0, \beta]$  by a discrete set of points  $G(\tau_i)$   $\tau_i = \frac{i\beta}{N_p}$   $i = 0 \dots N_p - 1$ , Then one introduces a discrete Hubbard Stratonovich field to linearize the interaction term and reduce the action Eq. (10) to a quadratic form. Then one traces over the Fermion field and the partition function then becomes a sum over Ising variables  $\sigma_i, i = 0, \dots, N_p - 1$ ,

$$Z = \sum_{\sigma_i} \det[A_{\uparrow}(\sigma_i)][A_{\downarrow}(\sigma_i)] . \quad (29)$$

Here A is the discretized version of the effective action after the U term is linearized by an Ising Hubbard Stratonvic transformation.

The discretized Greens function is also expressed as a sum over Ising variables,

$$G(\tau_l - \tau_{l'}) = \frac{\sum_{\sigma_i} \det[A_{\uparrow}(\sigma_i)][A_{\downarrow}(\sigma_i)] A^{-1}_{l,l'}}{Z} , \quad (30)$$

Most of the work was carried out with the Fye Hirsch algorithm which corresponds to a specific discretization of the functional integral,

$$A^{\mu}_{ll'} = \delta_{ll'} + e^{V_l^{\mu}} e^{-\Delta\tau\mu} \delta_{ll'+1} + e^{V_{l'}^{\mu}} \Delta_{l,l'} . \quad (31)$$

Here  $\mu = \uparrow, \downarrow$ ,  $\Delta_{ll'}$  is a discretized version of the Hybridization function in Eq. (15) and the antiperiodic delta function is defined by  $\delta_{ll'+1} = 1$  if  $l = l' + 1, l = 2, \dots, N - 1$ ,  $\delta_{ll'+1} = -1$  if  $l = l' = N$  and is zero otherwise. The quantities  $V_l^{\mu}$  are proportional to the Ising variables  $\sigma_l$ ,

$$V_l^{\mu} = \sigma_l \mu \text{arccosh}(e^{5\Delta\tau U}) . \quad (32)$$

All the sums are evaluated by importance sampling. To decide whether a Monte Carlo move from  $\sigma$  to  $\sigma'$  is accepted or rejected one needs the ratio of two determinants. This ratio is evaluated in terms of the local Green's function,

$$R \equiv \frac{\det[A(\sigma'_l)]}{\det[A(\sigma_l)]} = 1 + (1 - G(l, l))(e^{V_{l'}^{\mu} - V_l^{\mu}} - 1) . \quad (33)$$

When the move is accepted the new Green's function  $G'$  is given by

$$G'(l'', l') = G(l'', l') + (G(l'', l) - \delta_{l''l})(e^{V_{l'}^{\mu} - V_l^{\mu}} - 1) \frac{G(l, l')}{R} . \quad (34)$$

Other discretizations of the effective action such as

$$A^{\mu}_{l,l'} = \delta_{l,l'} + e^{V_l^{\mu}} e^{-\Delta\tau\mu} \delta_{l,l'+1} + 1 + \Delta_{l,l'} , \quad (35)$$

have been investigated<sup>35</sup> and they give comparable results. Therefore we concluded that a major improvement of the algorithm requires a discretization which is accurate to order  $\Delta\tau^2$ .

Typical values of L are 64 and 128 and 254. Typical values of  $\delta\tau$  is .25 which in practice restricts the simulations to inverse temperatures less than  $\beta$  of 64 .

We stress that there are two approximations in this scheme, the first has to do with the finite discretization of the greens function while the second has to do with the subsequent discretization of the functional integral. Both this approximations get better as  $\delta\tau$  goes to zero. In addition there is a source of error in the evaluation of the sum by importance sampling. This statistical error can be reduced by increasing the length of Monte Carlo run.

### 4.3 Exact diagonalization

The results of Section 2 allow us to apply exact diagonalization techniques on the *Anderson impurity model* in order to solve the large d problem. To use exact diagonalization methods one needs to produce: a) a correspondence between the exact  $G_0$  and an Anderson hamiltonian involving a finite number of conduction electron orbitals and b) a correspondence between the exact local Green's function  $G(i\omega_n)$  and  $G_0$  or the parameters of the Anderson impurity hamiltonian.

Once the correspondence a) is defined, one can carry out the operation illustrated on the upper box in Fig. 1. Given  $G_0$ , the correspondence a) assigns to it a unique Anderson impurity with a finite number of orbitals, i.e. a finite dimensional matrix whose green function  $G$  can be computed by standard exact diagonalization algorithms.<sup>46</sup>

Once the correspondence b) is established we can carry out the operation illustrated on the lower box in Fig 1. The  $G$  obtained by the methods described in the previous paragraph contains a large number of poles. The correspondence b) assigns to any Greens function  $G$  a  $G_0$  containing a finite (small) number of poles, i.e. an Anderson impurity model with a finite number of conduction electron orbitals.

Combining these two steps we obtain a discretized version of the mean field equations that converges to the exact answer as the number of orbitals is increased. Two algorithms differing mainly in step b) have been suggested.<sup>40,41,42</sup> We will describe here the algorithm of Ref. 42.

A  $G_0$  is parametrized by an Anderson model :

$$\begin{aligned}
 H = & \sum_{\sigma} \sum_{\rho=>,<} \left[ \left( \sum_{\alpha=1}^{N_C-1} a_{\alpha}^{\rho} c_{\alpha\sigma}^{\rho\dagger} c_{\alpha\sigma}^{\rho} + b_0^{\rho} (c_{\sigma}^{\rho\dagger} f_{\sigma} + h.c.) \right) \right. \\
 & + \left. \sum_{\alpha=1}^{N_C-2} (b_{\alpha}^{\rho} c_{\alpha\sigma}^{\rho\dagger} c_{\alpha+1\sigma}^{\rho} + h.c.) \right] + U(n_{f\uparrow} - \frac{1}{2})(n_{f\downarrow} - \frac{1}{2}) \\
 & + \sum_{\sigma} b_0 (f_{\sigma}^{\dagger} c_{0\sigma} + h.c.) .
 \end{aligned} \tag{36}$$

It contains two chains of conduction electrons and an extra orbital having zero energy.

The correspondence  $b$  is obtained by: decomposing the Green function  $G(z)$  into “particle” and “hole” contributions as  $G(z) = G^>(z) + G^<(z)$  with  $G^>(z) = \langle 0 | c \frac{1}{z - (H - E_0)} c^\dagger | 0 \rangle$  and  $G^<(z) = \langle 0 | c^\dagger \frac{1}{z + (H - E_0)} c | 0 \rangle$ , and expanding the respective contributions in a continued fraction expansion:

$$\langle f_0^{>/<} | \frac{1}{\omega \mp (H - E_0)} | f_0^{>/<} \rangle = \frac{\langle f_0^{>/<} | f_0^{>/<} \rangle}{z - a_0^{>/<} - \frac{b_1^{>/<2}}{z - a_1^{>/<} - \frac{b_2^{>/<2}}{z - a_2^{>/<} - \dots}}, \quad (37)$$

where  $|f_0^>\rangle = f^\dagger |gs\rangle$ ,  $|f_0^<\rangle = f |gs\rangle$  and  $|f_{n+1}\rangle = H|f_n\rangle - a_n|f_n\rangle - b_n^2|f_{n-1}\rangle$ ,  $a_n = \langle f_n | H | f_n \rangle$ ,  $b_n^2 = \frac{\langle f_n | f_n \rangle}{\langle f_{n-1} | f_{n-1} \rangle}$ ,  $b_0 = 0$ . This implies that  $G^>$  and  $G^<$  can be regarded as resulting from a Hamiltonian describing an impurity coupled to two chains with site energies  $a_n^{>/<}$  and hopping amplitudes  $b_n^{>/<}$ . Since the number of poles in the Green function is in general larger than the number of sites of the hamiltonian and the continued fraction is truncated to a given finite depth.

The approximation in this scheme relies on the fact that the continued fraction representation captures exactly the moments of the energy of the hamiltonian, up to the order retained in the continued fraction. It can thus be thought of as a moment by moment fitting. The extra site at the Fermi energy is introduced in order to better represent the low frequency region and, more importantly, to allow a feed-back of a metallic bath.

The hopping parameter  $\alpha = b_0/t^2$  is calculated by a single parameter minimization of the expression

$$\chi^2(\alpha) = \sum_{i\omega_n L}^{i\omega_n H} |G_A(i\omega_n, \alpha) - G(i\omega)|^2 \quad (38)$$

where now  $G_A(i\omega_n, \alpha) = \alpha/i\omega_n + (1 - \alpha)G_{N_C}(i\omega_n)$ .  $G_{N_C}$  is the truncated Green function to length  $N_C = N_{Site}/2$  and  $\omega_L$  and  $\omega_H$  are low and high energy cut-offs defined by the lowest poles of  $G$  and  $G_{N_C}$ , respectively. The coefficients  $a$  and  $b$  in Eq. (36) are obtained from the coefficients of the partial fraction expansion in Eq. (37).

#### 4.4 Perturbation theory

One of the advantages of dealing with a well studied impurity model, is that one can rely on a host of reliable approximate methods which have been specifically designed for treating this problem. At half filling Yamada and Yoshida<sup>27</sup> demonstrated that *for the Anderson impurity model* second order perturbation theory in  $U$  converged extremely well up to values of  $\frac{U}{D}$  of order 6. Georges and Kotliar implemented this scheme to study the large  $d$  Hubbard model.<sup>3</sup>

It was later shown<sup>14</sup> that this approach to the Hubbard model gives results in very good agreement with the quantum Monte Carlo results at finite temperatures. Furthermore they showed that this scheme gives the atomic limit results for large  $U$  and therefore it is an interpolating scheme valid for small and large  $U$ . The important insight is that the Anderson impurity problem is *analytic in  $U$*  irrespectively of the nature of the bath, so it can be treated perturbatively. The non analyticities, describing the lattice aspects of the problem, are brought in by the self consistency condition which is treated exactly by this method.

The results obtained with this method are useful because they provide a concrete analytic realization of the functional  $\Sigma_{imp}[G_0]$  and exhibits the functional form of  $G[G_0] \approx [G_0 - \Sigma_{imp}[G_0]]^{-1}$  defined in Section 2, and illustrates in a simple example the important role played by the self consistency condition. The perturbative calculation is very fast and allows us to scan the parameter space at low temperature. This task would be prohibitively expensive for current QMC or exact diagonalization algorithms.

To second order in perturbation theory the impurity self energy is given by:

$$\Sigma_{imp}[G_0](\tau) = -U^2 G_0^3(\tau) . \quad (39)$$

We can understand the success of this approximation for the following reasons: 1) It is good for weak couplings ( $U \ll t$ ) by construction, since the expansion is around  $U = 0$ . As shown by Yamada and Yosida (YY), it is able to produce not only the Abrikosov-Suhl resonance, but also the upper and lower incoherent bands as well. YY showed that the 4<sup>th</sup> order correction is two orders of magnitude smaller than the 2<sup>nd</sup> order contribution for the range of the interaction where the MIT occurs. 2) The atomic limit is exactly captured. When  $U$  is very large, and the system is deep in insulating side,  $G_0^{-1} \approx i\omega_n$ , the non-magnetic Hartree-Fock solution of the Green's function becomes exact,

$$G_L(i\omega) = \frac{1/2}{G_0^{-1}(i\omega_n) - U/2} + \frac{1/2}{G_0^{-1}(i\omega_n) + U/2} , \quad (40)$$

therefore, the self energy reads,

$$\Sigma = \left(\frac{U}{2}\right)^2 G_0(i\omega_n) \quad (41)$$

which is identical to the self energy that results from inserting  $G_0$  in Eq. (39) and Fourier transforming. Thus, the second order approximation is at least an interpolation scheme which becomes exact for both the  $U \rightarrow 0$  and  $U \rightarrow \infty$  limits.

#### 4.5 Other perturbative schemes

It is worthwhile to point out that before the mapping onto the Anderson impurity model had been carried out, the Hubbard model in large dimensions had been studied using fully self consistent perturbation theory and direct perturbation theory in  $U$ . Both schemes fail to give a Mott transition.<sup>54,55</sup>

Jarrell and coworkers have combined the NCA method with the self consistency condition to study various properties of the Hubbard model not too close to the Mott transition and report good agreement with the Quantum Monte Carlo results.

#### 4.6 The self consistent projective method

The self consistent impurity model near  $U_{c2}$  has two energy scales  $U$  and  $\Delta$ . The collapse of the scale  $\Delta$  causes unsurmountable numerical difficulties. To handle this problem the projective self consistent technique was introduced in Refs. 47 and 8. The idea is to eliminate the high energy configurations having scale  $U$  and simultaneously the high energy states of the bath of conduction electrons to obtain a problem containing a single energy scale  $\Delta$  which can then be easily handled with the methods of the previous subsections. This method is quite general, and is applicable to a large class of models of strongly correlated electrons where separation of scales takes place.

The one particle spectral function is decomposed into a sum of a low and a high energy part,  $\rho(\epsilon) = \rho^{low}(\epsilon) + \rho^{high}(\epsilon)$ .  $\rho^{low}(\epsilon)$  contains all states up to a cut-off that we take to be the Kondo temperature or renormalized Fermi energy of the half-filled Hubbard model and carries spectral weight  $\Delta$ ,

$$\Delta = \sum'_k 4V_k^2/D^2, \quad (42)$$

where the primed summation runs over the low energy states only.  $\rho^{high}(\epsilon)$  describes the upper and lower Hubbard bands, two atomic-like features at energy scales  $\pm U/2$ , and carries spectral weight  $1 - \Delta$ .

We can solve for  $\rho^{high}(\epsilon)$  using the techniques of the previous section. The main idea of the projective self-consistent approach is to eliminate the high energy states to obtain a low energy effective problem involving  $\rho^{low}$  only and thus containing only one energy scale. To carry out this program we separate the impurity configurations of the impurity Hamiltonian Eq. (14) into a low energy sector  $f_\sigma^\dagger|E\rangle$ , with eigenenergy  $-U/4$ , and a high energy sector  $|E\rangle$  and  $f_\uparrow^\dagger f_\downarrow^\dagger|E\rangle$ , with eigenenergy  $U/4$ , where  $|E\rangle$  denotes the empty configuration. Furthermore, as a result of the self consistency condition the conduction electron bath is divided into three bands (see Fig. 2): a metallic band centered around the Fermi energy, and semiconducting valence and conduction bands centered around energies  $\pm U/2$ . For the analysis of low energy properties, the valence and conduction bands can be taken as dispersionless, with the corresponding atomic states created by  $\eta_-^\dagger$  and  $\eta_+^\dagger$ , respectively.

We now eliminate the high energy impurity configurations and the high energy orbitals of the conduction electron bath, to obtain a low energy hamiltonian which we can use to calculate  $\rho_{low}$ . This is done using a canonical transformation which results in:

$$H_{eff} = \sum'_{kk'} J_{kk'} \vec{S} \cdot \vec{s}_{kk'} + \sum'_{k\sigma} \epsilon_k c_{k\sigma}^\dagger c_{k\sigma}, \quad (43)$$

where  $J_{kk'} = 8(V_k V_{k'}/U)[1 + 7(D/2U)^2(1 - \Delta)]$ ,  $\vec{S} = \frac{1}{2} \sum_{\sigma\sigma'} X_{\sigma\sigma'} \vec{\sigma}_{\sigma\sigma'}$  and  $\vec{s}_{kk'} = \frac{1}{2} \sum_{\sigma\sigma'} c_{k\sigma}^\dagger \vec{\sigma}_{\sigma\sigma'} c_{k'\sigma'}$ . Here,  $X_{\alpha\beta} \equiv |\alpha\rangle\langle\beta|$ , where  $|\alpha\rangle$  and  $|\beta\rangle$  are the eigenstates of the atomic Hamiltonian, are projection operators.

$H_{eff}$  corresponds to a Kondo problem coupling the atomic spin doublet to the low energy conduction electron bath.

The low energy part of the Green function can now be calculated directly from  $H_{eff}$ ,

$$G^{low}(i\omega_n) = - \int d\tau e^{i\omega_n \tau} \langle T_\tau F(\tau) F^\dagger(0) \rangle_{H_{eff}}, \quad (44)$$

where  $F_\sigma = e^S f_\sigma e^{-S}$  is the canonically transformed single particle operator and has the form

$$F_\sigma = \sum'_k \alpha_k [(X_{\sigma\sigma} - X_{-\sigma-\sigma}) c_{k\sigma} + 2X_{\sigma-\sigma} c_{k-\sigma}], \quad (45)$$

with  $\alpha_k = \frac{2V_k}{U} (1 + \frac{7}{4} \frac{D^2}{U^2} - \frac{7}{4} \frac{D^2}{U^2} \Delta)$ . The self-consistency equation for the low energy Green function then becomes,

$$\sum'_k \frac{4V_k^2/D^2}{i\omega_n - \epsilon_k} = G^{low}(i\omega_n). \quad (46)$$

The projective self-consistent method thus results in the closed set of Eqs. (43)-(46) which form the basis of our low energy analysis. The system contains only *one* energy scale,  $\Delta D$  and is therefore numerically tractable.<sup>47</sup> Some of the results of this method will be described in Section 6.

---

## 5. PHASE DIAGRAM AND THERMODYNAMICS

In the previous section we argued that the paramagnetic mean field equations have two classes of solutions: metallic when  $G(0) = -2i/D$  and insulating when  $G(0) = 0$ .

The qualitative distinction between a metal and an insulator is precise at zero temperature. At finite but small temperatures a sharp distinction between a metallic and an insulating solution can still be made, since we find a region where *two* solutions are allowed. One can be continuously connected to the  $T = 0$  metallic solution, and displays a peak like feature at the Fermi energy. The other solution can be connected to the  $T = 0$  insulating solution, and the Green's function extrapolates to zero at zero frequency. As the temperature is further increased this region of coexistent solutions disappears and we are left with a rapid crossover from a metallic

---

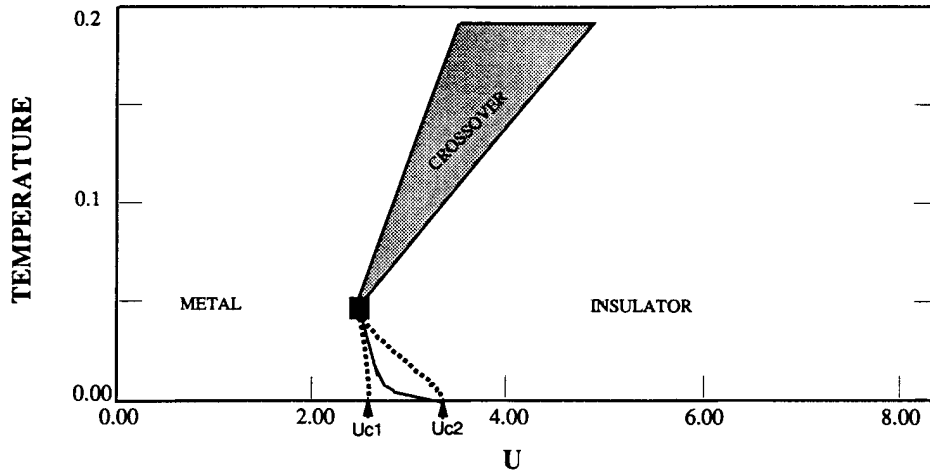


**FIGURE 4.** The phase diagram of the fully frustrated Hubbard model at half filling. It is possible to continuously move from one phase to the other since at high  $T$  the transition becomes a crossover. The solid line is obtained by comparing the free energies of the two solutions in the region where they are both allowed. The dashed lines indicate the region where the metallic and the insulating solutions coexist. The black square indicates the end of the 1<sup>st</sup> order line in a 2<sup>nd</sup> order point.

like solution to an insulating one. This is possible because at finite temperature there is no *qualitative* distinction between a metallic and an insulating state.

At zero temperature there are two critical values  $U_{c1}$  (the smallest  $U$  that allows an insulating solution) and  $U_{c2}$  (the largest  $U$  permitting a metallic solution) between which the mean field equations have two solutions. From these points two lines emerge in the  $U$ - $T$  plane of Fig. 4 which merge in a second order point. The area between the  $U_{c1}$  and  $U_{c2}$  lines is a coexistence region of metallic and insulating solutions. The actual transition takes place at an intermediate value  $U_c$  where the free energy of the two solutions cross. At zero temperature  $U_c = U_{c2}$ .<sup>42</sup>

In addition to the paramagnetic solution, the mean field equations in the broken symmetry phase may also have non trivial solutions. The range of parameters where the antiferromagnetic solution exists will depend on the details of the lattice structure and in particular on the degree of magnetic frustration.

To determine the phase diagram we then proceed in three steps: a) We first determine the region where the two paramagnetic solutions coexist. b) We then compare their free energy, their crossing determines the first order phase boundary between the paramagnetic metal paramagnetic insulator. c) Finally, when a Néel state is possible, we study the magnetically ordered phase and calculate the Néel

temperature to check whether the metal insulator transition found in step b) is preempted by a magnetic ordering transition.

In the paramagnetic phase the energy is computed from the Green's function by,

$$E = T/2 \sum_{nk} (i\omega_n + \epsilon_k) G_k(i\omega_n), \quad (47)$$

The entropy is calculated from,

$$S(T) = \int_0^T \frac{C_v}{T'} dT' + S(0), \quad (48)$$

where  $C_v$  is the specific heat and  $S(0)$  is zero for the metallic side and  $\ln(2)$  for the insulating side reflecting the double degeneracy of the paramagnetic insulating phase. The free energies of states are computed from

$$F = E - ST. \quad (49)$$

The qualitative phase diagram of the fully frustrated model in the limit of large  $d$  is shown in Fig. 4. It was obtained by the second order perturbation theory scheme. We checked that all the qualitative features such as the coexistence of metallic and insulating solutions at zero and finite temperatures, the existence of a line of first order phase transitions ending at a zero temperature quantum critical point and a finite temperature second order point, are genuine features of the large  $d$  Hubbard model by performing a few runs with the quantum Monte Carlo and exact diagonalization techniques described in Section 4. In the fully frustrated model the Néel temperature is suppressed to zero by the magnetic frustration, and we need only consider the paramagnetic phase.

It is worth noticing, the slope of the first order phase boundary is such that the insulator is reached upon heating. This reflects the fact that the paramagnetic insulator has higher entropy than the metal. It is a generic feature of the phase diagram of many strongly correlated systems. It ends in a critical point where a crossover region starts. This reflects the fact that the metal is sustained by activation across the Mott Hubbard gap, and as a result the slope of the crossover line between metal and insulator is  $T \approx U - D$ .

The phase diagram of a bipartite lattice such as the hypercubic lattice<sup>23</sup> or the Bethe lattice<sup>23</sup> is quite different. In this case, the low temperature metal to insulator transition discussed above is preempted by the onset of the Néel state. The phase diagram on the Bethe lattice is shown in Fig. 5.

It is clear that Slater's point of view is completely correct for understanding the metal to insulator transition *at very low temperatures in non-frustrated lattices* such as the Bethe lattice. The onset of antiferromagnetism makes the metal insulator transition within the paramagnetic phase completely irrelevant.

We finally turn to the phase diagram of a model having some intermediate degree of frustration. We studied a toy model, the two sublattice fully frustrated model

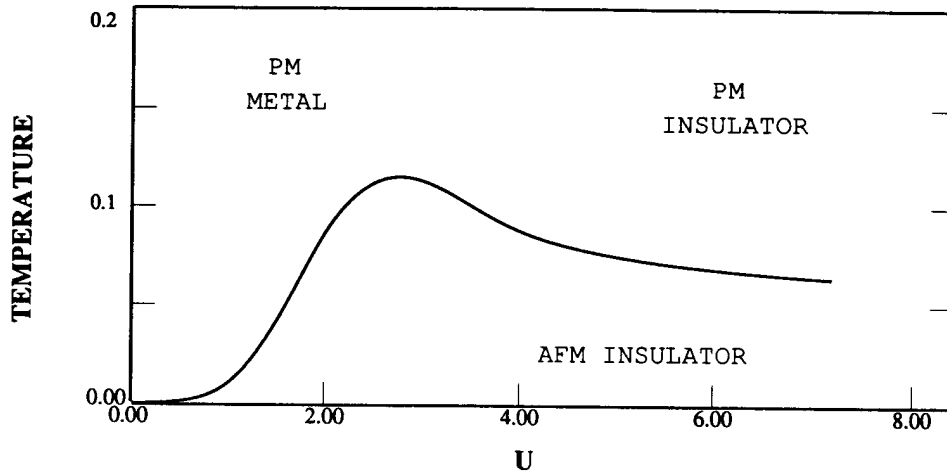


**FIGURE 5.** Phase diagram of the Hubbard model on a bipartite lattice at half filling. The thin line gives the Néel temperature of the regular Bethe lattice as a function of interaction  $U$ . The Néel temperature is much higher than the metal insulator transition temperature of the frustrated lattice. At high temperatures there is a smooth crossover between quasi metallic and quasi insulating behavior.<sup>18</sup>

(TSFFM), with values of  $t_1^2 = \frac{1}{4}t^2$  and  $t_2^2 = \frac{3}{4}t^2$ . but the general features are representative of more realistic frustrated lattices. The frustration dramatically reduces the Néel temperature. For large  $U$ , the Néel temperature is given by  $2(t_2^2 - t_1^2)/U$  while for small  $U$  we were able to obtain upper bounds to the Néel temperature to establish the relevance of the finite temperature metal insulator transition to this model. The  $T_{Neel}$  on the metallic side is smaller than the one on the insulating side and the antiferromagnetism occurs within the metallic phase. A schematic sketch of the phase diagram of the two sublattice fully frustrated model is shown in Fig. 6. We conclude that in the presence of moderate magnetic frustration, a paramagnetic insulator to paramagnetic metal transition takes place in purely electronic models.

The experimentally observed phase diagrams of transition metal oxides display incommensurate metallic magnetism. This can in principle be studied by extending the mean field theory to account for incommensurate phases as done by Freericks for the Falicov-Kimball model.<sup>30</sup> For this calculation to be meaningful, however, one should include the details of a realistic band structure of the transition metal oxide, which is beyond the scope of our work.

### 5.1 Thermodynamics

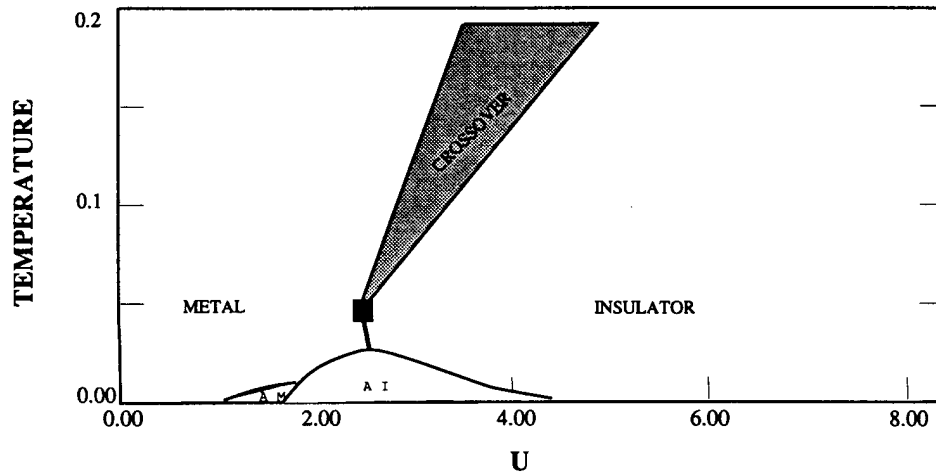


**FIGURE 6.** Schematic phase diagram of the two sublattice fully frustrated model with intermediate values of frustration  $t_1^2 = .25t^2$ ,  $t_2^2 = .75t^2$ .<sup>18</sup>

The mean field theory of strongly correlated electrons provides a powerful technique for studying the thermodynamics of strongly correlated electrons at finite temperatures. This is a significant improvement over earlier methods like the Gutzwiller variational approach or the slave boson method, which did not have satisfactory extensions to finite temperatures.

The main features of the thermodynamics in the strongly correlated metallic state can be understood from the existence of two energy scales.  $\Delta D$  the renormalized Fermi energy is also the scale for low lying spin fluctuations and  $U$ , the energy scale for charge fluctuations. For small  $U$  the two features coalesce while for large  $U$  only the activation across the upper Hubbard band exists.

Fig. 7 displays the specific heat  $C_v$  as a function of the temperature. In the strongly correlated metallic phase we find a separation of scales since  $\Delta$  is much smaller than  $U - 2D$ . At higher  $T$  a thermal activation peak appears at a scale  $U - 2D$  in both the metallic and insulating case. The linear in  $T$  Fermi liquid behavior is observed in the low temperature region, with the slope  $\gamma$  proportional to  $m^* \sim (U_{c2} - U)^{-1}$ .

The integral Eq. (48) gives the entropy as a function of temperature. The integral over the quasi-particle peak is equal to  $\ln 2$  while the integral over the second peak at around  $U - D$  contains the  $\ln 2$  entropy of the charge degrees of freedom.

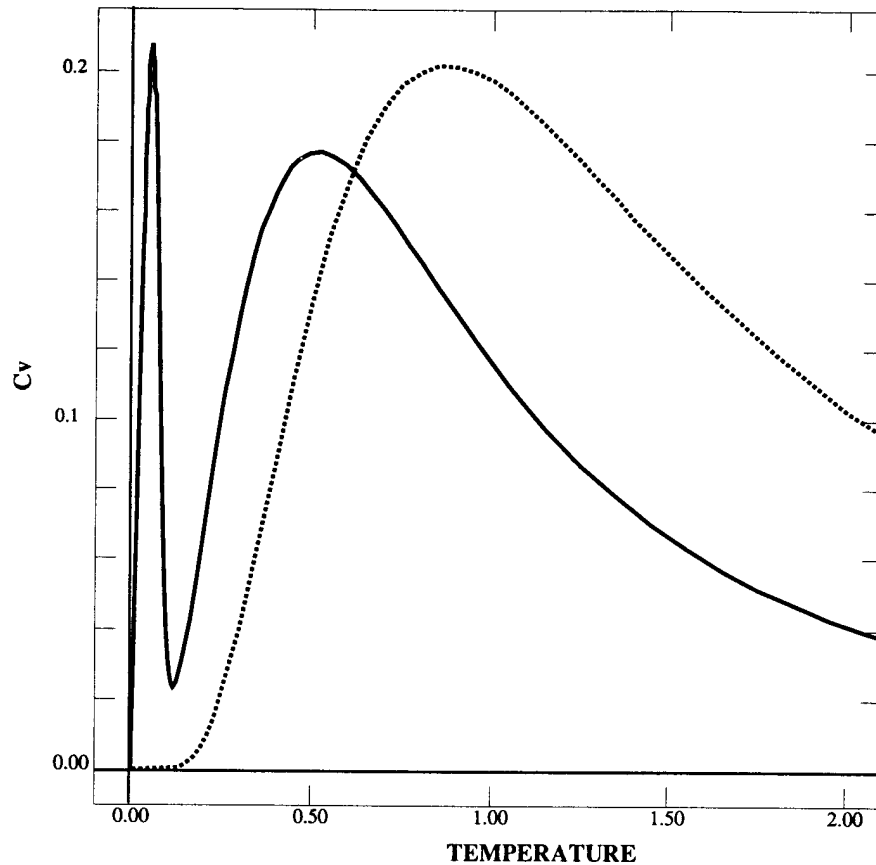


**FIGURE 7.** The specific heat  $C_v$  as a function of temperature. The solid line is for  $U = 2$  and the dashed line corresponds to  $U = 4$ . In the metallic case ( $U = 2$ ) it is apparent the separation of energy scales. The linear part, at low  $T$ , ends at  $T \sim \Delta$ , and the thermal activation of the incoherent features peaks at the bigger scale  $T \sim U - 2D$ . This last effect is the only one present in the insulating case.

## 6. THE ZERO TEMPERATURE METAL TO INSULATOR TRANSITION

In this section we investigate the fate of the metallic solution which was shown to be stable at zero temperature up to  $U_{c2}$ .<sup>42</sup> This investigation of the metallic phase is of interest in the light of the considerably large mass renormalizations observed in some transition metal oxides.

The destruction of the metallic state is driven by the collapse of the Fermi energy scale  $\Delta$  which we showed is proportional to  $U_{c2} - U$ . From the mean field equation  $G_0^{-1} = i\omega_n - t^2 G$ , we realize that this scale is also the *bandwidth* of the conduction electron bath which hybridizes with the local impurity in the Anderson model picture. It is easy to understand then, that for sufficiently large  $U$  this scale vanishes. Imagine solving the system of Eqs. (10), (11), and (12) by iteration. Consider a conduction electron bandwidth  $\Delta^n$  ( $W^n$  in the notation of<sup>23</sup>) at the  $n^{\text{th}}$  iteration step. For large  $U$ , solving the Kondo problem produces a bandwidth  $\Delta^{n+1} = e^{-U/t} \Delta^n$ . Therefore, the effective energy scale iterates to zero for  $n \rightarrow \infty$ .

Close to  $U_{c2}$ , there is a clear separation of energy scales and the local Green's function can be written as a sum of low energy and high energy parts:  $G_l$  and  $G_h$ . The high energy part resembles the solution of an atomic problem while the low energy part obeys a scaling form.

In terms of a spectral representation:

$$G_l = \int_{-\infty}^{\infty} \frac{\rho_l(\epsilon)}{i\omega - \epsilon} d\epsilon \quad (50)$$

$$G_h = \int_{-\infty}^{\infty} \frac{\rho_h(\epsilon)}{i\omega - \epsilon} d\epsilon \quad (51)$$

with the low energy part of the spectral density

$$\rho_l(\epsilon) = \frac{1}{t} f\left(\frac{\epsilon}{\Delta}\right) \quad (52)$$

exhibiting a scaling form as  $\Delta \propto U_{c2} - U$  goes to zero.  $\rho_h(\epsilon)$  describes the high energy non scaling parts (Hubbard bands) centered around  $\pm U/2$ . A somewhat oversimplified but transparent picture of the spectral function is obtained by taking  $\rho_h$  to be two semi-circles with overall weight  $1 - \Delta/D$ ,  $t = D/2$ .

The one particle spectral function is shown in Fig. 3. Notice that the Mott Hubbard gap is well developed by the time that  $U$  is close to  $U_{c2}$ .

The scaling function  $f$ , which resolves the low energy peak in Fig. 3 was calculated in Ref. 47 by using the methods of Section 4.6,

$$\Sigma(i\tilde{\omega}_n) = -1.7i\tilde{\omega}_n - i1.1(i\tilde{\omega}_n)^2. \quad (53)$$

Here  $\tilde{\omega}_n = \omega_n/\Delta$ . The term of the self-energy linear in  $i\tilde{\omega}_n$  implies a quasi-particle residue  $z \equiv (1 - \partial\Sigma/\partial i\omega_n)^{-1} = \Delta/1.7$  which vanishes as the critical point is approached. The momentum-independence of the self-energy in turn leads to a quasi-particle mass  $m^*/m = 1/z = 1.7$ , and a linear coefficient of the specific heat,

$$\gamma = 1.7 \frac{4\pi k_B^2}{3} \frac{1}{D\Delta} \quad (54)$$

which diverges at the critical point.

The imaginary part of the self-energy, at low energies, is quadratic in frequency and has a stronger divergence than the quasiparticle residue.

$$\text{Im}\Sigma(\omega + i0^+) = -\frac{1.1 \omega^2}{\Delta^2 D} \quad (55)$$

at the critical point.

All this is reminiscent of the Brinkman-Rice scenario of the Mott transition.<sup>21</sup> This early approach captured the essential physics of the model: the collapse of the renormalized Fermi energy as a result of the proximity to a localization transition, that does not favour a particular form of magnetic long range order (i.e. the magnetic susceptibility is  $q$  independent).

The mean field approach goes beyond the variational wave function method and allow us to extract lifetimes and other dynamical information. It also has a simple extension to finite temperatures as described in Section 4.

There are however some significant differences. The double occupancy  $\langle n \uparrow n \downarrow \rangle$  does not play the role of an order parameter and is finite at the Mott point. This can be understood by the relation between the average local moment  $\langle n \uparrow n \downarrow \rangle$  and the double occupancy  $\langle n \uparrow n \downarrow \rangle$ :

$$1 - \langle (n \uparrow - n \downarrow)^2 \rangle = \langle n \uparrow n \downarrow \rangle \quad (56)$$

Even in the insulator the local moment is less than 2 because of virtual quantum fluctuations. This implies that the double occupancy is finite, as shown in Fig. 8. Note however that the doubly occupancy is relatively small (of the order of a few percent) near the Mott point.

A local spin spin autocorrelation function offers a different view of the transition. As we approach the Mott point the local spin-spin autocorrelation function  $\langle m_z(\tau)m_z(0) \rangle$  develops long term memory,

$$\langle m_z(\tau)m_z(0) \rangle \approx e^{-\tau\Delta D} \quad U < U_{c2} . \quad (57)$$

While in the insulating side

$$\lim \langle m_z(\tau)m_z(0) \rangle = m_0 > 0 \quad U > U_{c2} \quad (58)$$

The *local charge* susceptibility is finite (and non zero) at the transition. This can be checked by calculating directly the charge susceptibility of an Anderson impurity in an insulating medium in an expansion in  $\frac{t}{U}$ .

The local and the  $q=0$  susceptibilities exhibit very different behavior. This can be understood very simply using the connections between the large  $d$  Hubbard model and the impurity model. As shown in Section 2 the local correlation functions of the large  $d$  Hubbard model are those of the associated impurity model. Since the local spin-spin correlation function displays a broken ergodicity, the local susceptibility,  $\chi_{Local}^s = \int_0^\beta \langle m_z(\tau)m_z(0) \rangle d\tau$ , diverges as we approach the Mott point:

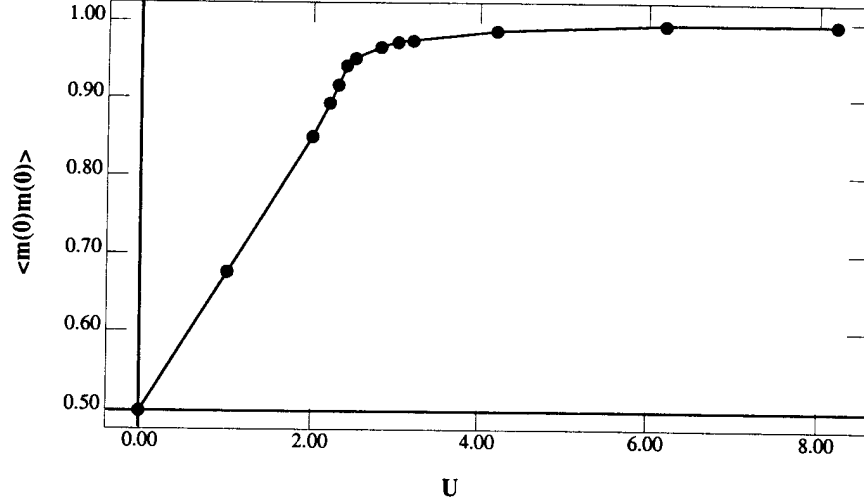


FIGURE 8.  $\langle m^2 \rangle$  as a function of interaction strength.<sup>14,18</sup>

$$\chi_{Local}^s \approx \frac{1}{\Delta}. \quad (59)$$

The  $q = 0$  susceptibility is calculated by applying an external magnetic field on the impurity and solving the self consistency equations for the bath and the Green's functions *in the presence of a field*. Then one computes the ratio of the induced magnetization to the applied magnetic field. The uniform susceptibilities differ from the local ones because of the polarization of the Weiss field due to the external perturbation. We will illustrate how this effect, which is at the heart of the Fermi liquid theory, modifies the  $q = 0$  response functions near  $U_{c2}$ .

In the presence of a small chemical potential away from the particle hole symmetric value and a small magnetic field the mean field equations are,

$$G_{0\sigma}^{-1} = i\omega_n + \mu + \sigma h - t^2 G_{\sigma}. \quad (60)$$

To illustrate this effect we use an approximate analytic parametrization of the numerical results. The high frequency part of the Green's function is polarized like a local moment which can be described as a superposition of Hartree Fock solutions. It has been demonstrated that as  $U \sim U_c$  the upper and lower Hubbard bands are well developed, so that for low frequencies and fields, a good approximation for  $G_{\sigma}$  is,

$$G_{\sigma} = \frac{n_{\sigma}}{[i\omega_n - \frac{U}{2}]} + \frac{n_{-\sigma}}{(i\omega_n + \frac{U}{2})} + \frac{2}{D} \frac{\Delta}{i\omega_n + \Delta(\text{sig}\omega_n)}. \quad (61)$$

Inserting Eq. (61) in Eq. (60), we have for small frequencies,

$$G_{\sigma\sigma}^{-1} = i\omega_n + \mu + h\sigma + 2\frac{t^2 m_\sigma}{U}\sigma. \quad (62)$$

Where  $n_\sigma = n + \frac{m_\sigma}{2}$ . Eq. (62) describes an impurity problem in the presence of an external field  $h_{eff} = h - 2\frac{t^2}{U}m_\sigma$ . We can compute the magnetization from the theory of the Anderson impurity model in an effective field  $h_{eff}$ . We know that  $m = \chi_o h_{eff}$  with  $\chi_o \sim \frac{1}{\alpha T_k}$ ,  $T_k$  is the effective Kondo energy of the problem which in our case corresponds to  $\Delta$ , and  $\alpha$  a numerical coefficient of order unity. Solving for  $m$  we find,

$$\chi_s = \left[ \frac{dm}{dh} \right]_{h=0} = \frac{1}{[\chi_o^{-1} + 2\frac{t^2}{U}]} = \frac{1}{\alpha\Delta + J_o}, \quad (63)$$

where we have defined the magnetic exchange energy  $J_o = 2\frac{t^2}{U} (= \frac{D^2}{2U})$ .

The physical interpretation of this equation is transparent: the exchange arises from high energy processes which are largely unaffected by the Mott transition. As a result the susceptibility varies continuously, as  $U$  passes through  $U_c$ . The result in Eq. (63) should be compared with Eq. (59).

Similar considerations apply to the charge susceptibility. Applying a chemical potential does not cause a change (to order  $\delta n$ ) in the distribution of integrated spectral weight between the upper and lower Hubbard bands. This can be readily understood by extending the observation of<sup>23</sup> that the high energy features are correctly reproduced by an expansion around the atomic limit. In this limit a small particle hole asymmetry shifts the energies of the atomic levels but does not transfer spectral weight. The change in the low energy part of the Green's function is easily estimated using Fermi liquid theorems. The change in  $G(0)$  as a result of a change in chemical potential is given by the phase shift which in turn is given by the shift of the location of the center of the resonance. Its width, does not change to order  $\Delta$  because of particle hole symmetry. Assuming that at low frequencies the result of applying  $\mu$  is to shift the center of the resonance by  $\epsilon_f$ :

$$G(i\omega_n) \simeq \frac{\Delta}{(i\omega_n + \epsilon_f + i\Delta \text{sig}\omega_n)}, \quad (64)$$

with  $\delta n \simeq \frac{\epsilon_f}{\pi\Delta}$ . We find  $\delta G(0) = \frac{\delta n}{\Delta}$  and therefore, from Eq. (60), the effective chemical potential seen in the impurity model is  $\delta\mu_{eff} = \delta\mu - \frac{t^2}{\Delta}\delta n$ . The response of the impurity to this shift in the chemical potential is  $\delta n = \chi_{imp}\delta\mu_{eff}$  with  $\chi_{imp} \simeq \frac{1}{U}$  the charge susceptibility of the impurity. Combining these equations we obtain:

$$\frac{\delta n}{\delta\mu} = \frac{\chi_c^0}{(1 + \frac{\chi_c^0 t^2}{\Delta})} \simeq \Delta, \quad (65)$$

which is the charge susceptibility that vanishes as  $(U_c - U)$  as we approach the Mott transition.

The comparison of the kinetic energy  $T = \langle \sum_k \epsilon_k c_k^\dagger c_k \rangle = \sum_{nk} \epsilon_k G_k(i\omega_n)$  and the potential energy  $V = U \sum \langle n_\uparrow n_\downarrow \rangle$  of the two metallic and the insulating solution at zero temperature reveals that the difference in the internal energy of the two states is much smaller than the corresponding difference in the kinetic and potential energy. The gain in kinetic energy by delocalization is almost perfectly cancelled by the loss in potential energy due to the Coulomb repulsion in doubly occupied sites. Recently using the methods of Section 4.3 Rozenberg et. al. established that for the semicircular density of states, the zero temperature metal to insulator transition takes place at  $U_{c2}$  that is the metal has always lower energy than the insulator. Furthermore, the near degeneracy of the metallic and the insulating state near  $U_{c2}$  follows from the bifurcation of two stationary points of the free energy energy functional, the free energy difference between these states is given by:

$$E_M - E_I \approx (U - U_{c2})^3. \quad (66)$$

This is different from the Gutzwiller result where the energy difference is proportional to  $\Delta^2$ .<sup>39</sup>

We conclude that the Hubbard model in large dimensions therefore, supports the Brinkman Rice scenario for the destruction of the metal, and eliminates many of the deficiencies which were due to the use of an *approximate* variational wavefunction.

A natural scenario for the destruction of the insulating solution would be a simultaneous narrowing of the gap of the insulator. This would have been a realization of the original Hubbard scenario for the MIT driven by the closing of the upper and lower Hubbard bands. This would imply a divergence of the dielectric constant when the transition is approached from the insulating side. This scenario is indeed realized in large dimensions but at a smaller value of  $U$ ,  $U_{c1} \approx 2D$ .<sup>42</sup>

---

## 7. COMPARISON WITH EXPERIMENTS

Besides combining, extending and putting in perspective the old scenarios and ideas, the mean field theory predicted a couple of surprising results. The first one is the phase diagram of the frustrated Hubbard model at Half filling, featuring a finite temperature second order point a line of first order transitions at low temperatures and a crossover region at higher temperatures.

While some of these features arose in earlier studies. Most noticeably in the mapping of the Hubbard model onto the Emery Blume Griffith model, by Castellani et. al.,<sup>34</sup> and the finite temperature extensions of the Gutzwiller approach by Spalek and collaborators<sup>37</sup> and by Kotliar and Ruckenstein,<sup>36</sup> a comprehensive treatment had been missing.

The second surprising of the large  $d$  solution is the prediction of a second order Mott transition at zero temperature which is driven by the collapse of an energy scale the Fermi energy, while the Mott Hubbard gap is already well formed. This is

---

a necessary consequence of the existence of two critical values of the interactions. At  $U_{c1}$  the insulator disappears when the Hubbard bands close (Hubbard scenario). Since  $U_{c1} < U_{c2}$  near  $U_{c2}$  the Hubbard bands are well separated from the low energy quasiparticles.

We will now examine some experiments on three dimensional transition metal compounds in the light of the mean field theory results discussed earlier. One should keep in mind, however, that in most transition metal compounds the correlated electrons in the d orbital are degenerated, and this degeneracy has not been included in the present version of the Hubbard model. The mean field theory can be extended in a straightforward manner to a degenerate Hubbard model. We note however that this extension, will not change the qualitative features of the Mott transition, while it may be very important in predicting the correct magnetic and orbital order in the insulating phase.

The phase diagram obtained in Fig. 6 has a striking qualitative resemblance to the features of the phase diagram of  $V_2O_3$  provided that we identify the ratio  $U/D$  with pressure. This system was studied extensively before, and has been revisited again most recently by Carter.<sup>24</sup>

On a qualitative level, we find that the overall agreement between the predicted phase of the model and what is experimentally observed is quite good. There is a first order metal insulator transition at finite temperature ending in a second order point. At higher temperatures there is a sharp crossover line with the opposite slope as observed in Ref. 38. The Hubbard model by itself, can therefore produce the three phase boundaries, antiferromagnetic insulator to paramagnetic metal, (AFI-PM), paramagnetic metal to paramagnetic insulator, (PM-PI), paramagnetic insulator to antiferromagnetic insulator, (PI-AFI), and the cross-over regime observed in nature. Interestingly, we also found, in the two sublattice fully frustrated model within a Hartree-Fock approximation, a small region of metallic antiferromagnetic state similar to the experimental observation of.<sup>24</sup> We expect that the details of the antiferromagnetic metallic phase will be very sensitive to the details of the band structure of the system. The application of the mean field theory to a model having the realistic band structure of  $V_2O_3$  seems right now very promising.

Some of the features of the  $V_2O_3$  phase diagram appear in other strongly correlated systems which undergo a metal insulator transition as a function of pressure. A more recent example is the  $NiI_2$  system where the metal insulator transition is known to be *isostructural*.<sup>33</sup> Furthermore the phase diagram of He 3 is qualitatively similar if we identify the solid phase with the paramagnetic insulator phase and the liquid phase with the metal. Therefore the pressure induced first order metal to insulator transition upon *heating* or upon decreasing pressure seems a very general feature of correlated Fermions which can be accounted for by a simple electronic model and need not be driven by the Fermion lattice interaction.

The two phase (metal insulator) coexistence region and the high temperature metal insulator crossover have been observed in  $V_2O_3$ .

Photoemission experiments are the most direct probe of the one electron spectral function. In a recent paper Fujimori et al.<sup>29</sup> have examined the spectral function of several transition metal compounds with a (slightly distorted) cubic perovskite

structure containing 1 d electron for transition metal. In these systems the value of  $U_{eff}/D$  changes because the distance between the transition metal ions changes with distance. They range from ,  $ReO_3$  to  $YTiO_3$  which is clearly insulating. The photoemission spectra clearly shows that the  $LaTiO_3$  is very close to the Mott transition point, and that the weight in the low energy part of the spectrum vanishes by the time the the lower Hubbard band is well formed, in complete agreement with the conclusions of Section 6 and Fig. 3.

Recent optical conductivity studies in the  $NiI_2$  system confirms this point of view. The evolution of the optical and the dc conductivity was studied as a function of the pressure.<sup>32</sup> This study reveals that at the metal insulator transition, determined from the dc conductivity studies the, optical gap is finite. Since the optical gap is less or equal than the one particle gap these experiments are consistent with the photoemission results.

The  $LaTiO_3$  is a particularly interesting system. When stoichiometric it is poised at the brink of the Mott transition. By substituting Sr by La one can move away from the Mott point thus producing a three dimensional analog of the  $La_{2-x}Sr_xCuO_2$  system .

The system  $La_{1-x}Sr_xTiO_3$  as a function of doping  $x$  was recently studied by in a beautiful set of experiments by the group of Tokura et al.<sup>25</sup> They measured the specific heat coefficient  $\gamma$  the susceptibility resistivity and Hall number as a function of  $x$ .

The resistivity is proportional to the square of the temperature  $\rho = AT^2$  demonstrating that these systems are Fermi liquids. Moreover the coefficient A is enhanced as we approach the Mott transition furthermore A scales as *the square* of the linear term of the specific heat  $\gamma$ .

Their results show that both  $\chi$  and  $\gamma$  are enhanced as they approach the Mott transition their ratio remains finite. Furthermore , the Hall coefficient is electronlike and is in rough agreement with the (large) volume of the Fermi surface.

Since the photoemission study shows that the  $x = 0$  point is close to the Mott transition,<sup>29</sup> we picked  $U = 3.2D$  and run our quantum Monte Carlo to calculate  $\gamma$  vs. doping. The results are shown in Fig. 9, together with the experimental data of Tokura et. al. The agreement is quite good.

We can therefore take over the analysis of Section 6 and take  $\Delta \approx xD$  as the energy scale which is collapsing at the Mott point.

The mean field theory results allows us to understand the scaling of A with  $\gamma^2$ . Furthermore the coefficient of proportionality can be estimated by converting the  $\omega^2$  dependence at zero temperature to a  $(\pi T)^2$  dependence at zero frequency and finite temperature. Using the Kubo formula for the conductivity without vertex corrections, on the hypercubic three dimensional lattice , we find a resistivity  $\rho(T) = AT^2$  where  $A = -\frac{\pi^{5/2}\hbar a}{e^2 D} \frac{\partial^2 \Sigma(i\omega_n)}{\partial (i\omega_n)^2}$  giving rise to a finite ratio,

$$\frac{A}{\gamma^2} = 8.2 \times 10^3 a \text{ (}\Omega m\text{)} , \quad (67)$$

where  $a$  is the hypercubic lattice spacing in units of meter. For  $Sr_{1-x}La_xTiO_3$  with  $x = 0.9$ , which is close to the Mott transition, Eq. (67) yields  $A/\gamma^2 = 4.4 \cdot 10^{-6} \Omega m$

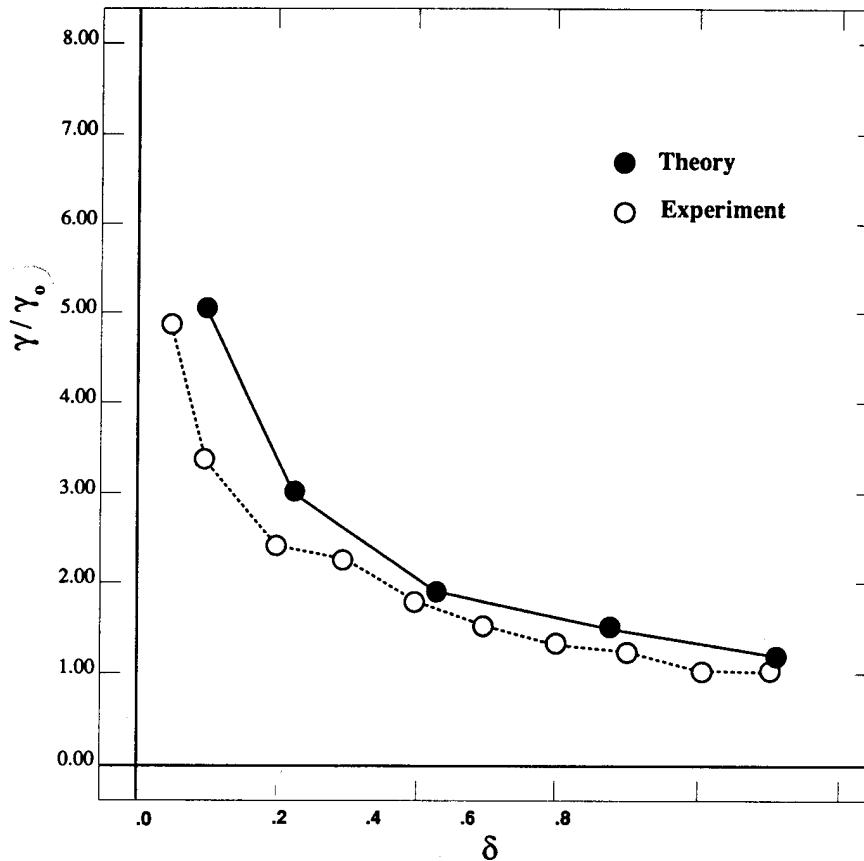


**FIGURE 9.** Comparison to experimental observation of the linear coefficient of the specific heat  $\gamma$  as a function of doping for an inverse temperature of  $\beta = 32$ . Experiment from Ref. 25. The  $U$  is assumed to be close to  $U_{c2}$  and the bandwidth is determined from the large doping weak correlation limit.

when we use  $a = 8.3 \times 10^{-10} m$ . This result is in good agreement with the measured value  $A/\gamma^2 = 8 \times 10^{-6} \Omega m$ .<sup>25</sup>

The enhancement of the susceptibility and the constant value of the  $\frac{\chi}{\gamma}$  ratio can be understood provided the value of the exchange constant  $J$  in Eq. (63) is not too large and one does not approach the transition too closely. This interpretation is highly plausible since the Néel temperature in  $LaTiO_3$  is of the order of a 150 degrees and the smallest doping measured is  $x = .05$ .

Finally, the term of the imaginary part of the dynamical spin susceptibility linear in frequency is given by:

$$\lim_{\omega \rightarrow 0} \frac{\chi''_s(\omega + i0^+)}{\omega} = 41/(D\Delta)^2. \quad (68)$$

This allows us to predict that the NMR relaxation rate diverges as the square of the specific heat.

The qualitative agreement between existing experimental data, in  $V_2O_3$ ,<sup>24</sup>  $NiI_2$  and in  $La_{1-x}Sr_xTiO_3$ <sup>25</sup> lead us to believe that the Hubbard model treated by what appears to be the correct (at last!) mean field theory is at least a qualitatively correct model for describing these systems. Moreover adding some realistic features, like a realistic density of states, crystal structure and atomic orbitals, can result, in the first ab initio first principles description of correlated transition metal oxide systems.

---

## 8. CONCLUSIONS

As discussed in Section 6 the solution of the Hubbard model in the limit of large dimensions has provided a consistent description of the Mott transition where various early ideas transition can be put in perspective.

An important open question is what happens to the transition at finite dimensions? We expect that the Mott transition and the metal charge transfer insulator transition are in the same universality class. The large N expansion results of Ref. 28 indicates that for  $N = 2$ ,  $U_{c1}$  and  $U_{c2}$  coincide and that the Mott transition is second order with continuous disappearance of the Kondo resonance and a gradual closing of the Mott gap.

Similar results were obtained with the slave boson approach to the Hubbard model. Whether the large N expansion is missing crucial  $1/N$  terms which would split the two transitions, or whether the  $1/d$  corrections would bring the two transitions to one, remains an interesting open problem.

As discussed in Section 7 the mean field approach seems to be a reliable tool for understanding many experiments in three dimensional transition metal oxides. The use of impurity models to model the photoemission in correlated electron systems is widely use. Since the self consistency condition described in Section 2 is very simple to implement we expect that the mean field method will become the tool of choice for describing photoemission experiments.

The dramatic difference between the behavior of the three dimensional system  $La_{1-x}Sr_xTiO_3$  and the quasi two dimensional  $La_{1-x}CuO_4$  raise many questions in the light of the results in Sections 6 and 7. The two systems are so similar in many respects that their differences should teach us something about what is unique to the copper oxide layers. The  $La_{1-x}Sr_xTiO_3$  system behaves as the mean field theory predicts, this is canonical Mott Hubbard behavior. To understand their differences various possibilities come to mind: 1) The most obvious one is that

dimensionality is very important. Three dimensional systems behave very closely to the mean field theory predictions. Two dimensions is special, and there mean field theory fails. 2) The relative size of the magnetic exchange to the hopping is important. The  $La_{1-x}Sr_xTiO_3$  has a Néel temperature of 150 K and we estimate 25K for the exchange constant in Eq. (63) by treating the insulating phase as a three dimensional Heisenberg model within mean field theory. The  $La_{1-x}CuO_4$  has an exchange constant of 1500K, an order of magnitude larger.

The mean field theory does not capture the effects of the local exchange because the individual  $J$  along a bond is of order  $1/d$ . Spin waves are also outside the scope of a mean field prediction. Furthermore the coupling between quasiparticles and collective modes is also down by powers of  $\frac{1}{d}$  and therefore absent in the mean field theory. This would explain the success of the mean field in the case  $La_{1-x}Sr_xTiO_3$  and its failure for  $La_{1-x}CuO_4$  where magnetic exchange plays a more dominant role.

3) A third possibility is that the Hubbard model does not capture the essential physics of the  $La_{1-x}CuO_4$  system. This point of view has been put forward forcefully by several authors<sup>41,42</sup> using a variety of approaches. The mean field theory applied to multiband systems containing explicit copper and oxygen orbitals has already yielded results quite different from the Hubbard model.<sup>11,6</sup>

I believe that 2) is the most likely explanation and this motivates us to carry out various extensions of the mean field framework to capture magnetic correlations. We mention several directions. A loop expansion around the mean field theory has been formulated and carried out in a functional integral framework in the presence of disorder.<sup>51</sup> The single site mean field theory can be extended to larger clusters, in exact analogy to the Bethe Peierls extension of the Weiss mean field theory.<sup>45</sup> Finally I suggest models where the charge charge and the spin spin interactions are scaled as  $\frac{1}{\sqrt{d}}$  (instead of the trivial  $\frac{1}{d}$  scaling which results in Hartree Fock theory) to allow for a non trivial coupling between the quasiparticles to charge and spin density modes.

These and many other extensions improvements and applications of the mean field framework will be carried out in the near future.

---

## APPENDIX I

$H_{eff}$  in Eq. (2) is the sum of the original *local* term in Eq. (1)  $s_0 h_0$  plus the generating functional of the connected correlation functions of a cavity hamiltonian  $H_c$  (the hamiltonian (1) with site zero removed), in the presence of external sources  $J_i \equiv J_0 i S_0$ .  $H_{eff} = const + \sum_{r=1}^{\infty} \frac{1}{r!} J_{i_1} \dots J_{i_r} \langle S_{i_1} \dots i_r \rangle_{H_c}^c$ . In a ferromagnetic system when  $J_{ij}$  is scaled as  $\frac{1}{d^{|i-j|}}$  where  $|i-j|$  is the Manhattan distance between  $i$  and  $j$ , only the one point function survives the  $d \rightarrow \infty$  limit and,

$$H_{eff} = h + \sum_i J_{oi} \langle S_i \rangle_{(o)} . \quad (69)$$

We consider the hypercubic lattice in the limit of large coordination and we scale  $J_{ij}$  as  $\frac{J}{2d}$ . In this case the expectation value of the magnetization calculated with the cavity hamiltonian,  $\langle S_i \rangle_{H_c}$  equals the magnetization at site 0 calculated with the original hamiltonian and the effective field is given by,

$$h_{eff} = h + Jm . \quad (70)$$

## APPENDIX II

We obtain a formal expression for  $S_{eff}$  by introducing a cavity lagrangian  $\mathcal{L}_2$  as follows  $L = \mathcal{L}_l(o) + \mathcal{L}_2 + L_{source}$ :

$$\mathcal{L}_2 = \sum_{i \neq o} \mathcal{L}_l(i) - \sum_{i \neq j \neq o} \int_0^\beta t_{ij} (c_i^\dagger c_j + c_j^\dagger c_i) , \quad (71)$$

with

$$\mathcal{L}_l(i) = c_i^\dagger \left( \frac{\partial}{\partial \tau} + \mu \right) c_i + c_{i\uparrow}^\dagger c_{i\uparrow} c_{i\downarrow}^\dagger c_{i\downarrow} , \quad (72)$$

and

$$L_{source} = \bar{\eta}_i c_i + c_i^\dagger \eta_i , \quad (73)$$

where the sources are given by  $\bar{\eta}_i = t_{i0} c_0^\dagger$  and  $\eta_i = t_{i0} c_0$ .

We calculate  $S_{eff}$  by viewing Eq. (10) as the sum of the local part of  $L$ ,  $\mathcal{L}_l(o)$  and the generating functional of the connected Green's functions,  $\tilde{G}_r$  of the cavity Lagrangian  $\mathcal{L}_2$  which describes a Hubbard model with a site removed.

$$S_{eff} = \sum_{r=1}^{\infty} \int [\bar{\eta}_{i_1}(\tau_{i_1}) \dots \bar{\eta}_{i_r}(\tau_{i_r}) \eta_{j_1}(\tau_{j_1}) \dots \eta_{j_m}(\tau_{j_m}) \tilde{G}_r(\tau_{i_1}, i_1 \dots \tau_{i_r}, i_r \tau_{j_1}, j_1 \dots \tau_{j_r}, j_r)] + \mathcal{L}_l(o) \quad (74)$$

**Bethe lattice.** In the Bethe lattice the removal of the site at the origin force all the spatial indices in Eq. (74)  $i_1 = \dots = j_r$  to collapse and,

$$\tilde{G}_r(\tau_{i_1}, i_1 \dots \tau_{i_r}, i_r \tau_{j_1}, j_1 \dots \tau_{j_r}, j_r) = \delta_{i_1, 1} \dots \delta_{j_r, 1} (m+1) t^{2r} \Gamma_r[\tau_{i_1} \dots \tau_{i_r} \tau_{j_1} \dots \tau_{j_r}] . \quad (75)$$

The functions  $\Gamma_r$  can be calculated from the connected correlation functions of a Lagrangian describing the effective action for a site 1, when his neighbor zero is removed  $\mathcal{L}_{0,1}$ ,

$$\mathcal{L}_{0,1} = \mathcal{L}_l(1) + m \sum_n t^{2n} c_1^\dagger(\tau_1) \dots c(\tau_{j_r}) \Gamma_r[\tau_{i_1} \dots \tau_{i_r} \tau_{j_1} \dots \tau_{j_r}] . \quad (76)$$

The recursive structure on the Bethe lattice then imply that,

$$\Gamma_r[\tau_{i_1}, i_1 \dots \tau_{i_r}, i_r \tau_{j_1}, j_1 \dots \tau_{j_r}, j_r] = \langle c^\dagger \dots c^\dagger c \dots c \rangle_c [\mathcal{L}_{0,1}] . \quad (77)$$

Here the subscript indicates a *connected* correlation function calculated with weight  $[\mathcal{L}_{0,1}]$ .

**Limit of large spatial coordination.** We scaled  $t_{ij} \sim (\frac{1}{\sqrt{d}})^{|i-j|}$  so  $\tilde{G}_j \sim (\frac{1}{\sqrt{d}})^{|i-j|}$  in the large  $d$  limit the first term in Eq. (74) is of order 1. The second term involves a *connected* point function  $\tilde{G}_{ijkl}$  with falls off as  $(\frac{1}{\sqrt{d}})^{|i-j|} (\frac{1}{\sqrt{d}})^{|i-k|} (\frac{1}{\sqrt{d}})^{|i-\ell|}$ . While there are four sums which give  $d^4$ , and four factors of  $t$  giving  $\frac{1}{d^2}$ . Since  $|i-j|$  is at least 2 the net result is of order  $\frac{1}{d}$ . In general the  $n$ th order term in Eq. (74) is of order  $\frac{1}{d}^{n-2}$  so only  $n = 2$  survives the  $d \rightarrow \infty$  limit. providing an explicit expression for the effective action and the Weiss field in Eq. (10):

$$-G_o^{-1} = \frac{\partial}{\partial \tau} + \mu + \sum_{ij} t_{oi} t_{oj} \tilde{G}_{ij} , \quad (78)$$

$\tilde{G}_{ij}$  is the Green's function of the Hubbard model with site  $o$  removed.

Equation (78) relates the Weiss field  $G_0$  to the Green's function of a Hubbard model with one site removed. A second simplification of the limit of infinite dimensions is the occurrence of a simple relation between the cavity Green's function and the local Green's function of the Hubbard model,

$$\tilde{G}_{ij} = G_{ij} - \frac{G_{io} G_{oj}}{G_{oo}} . \quad (79)$$

This equation which already appears in Ref. 20 can be proved by expanding both sides in powers of  $t_{ij}$ .

Notice at this point that in the paramagnetic state of the large  $d$  Bethe lattice  $\tilde{G}_{ij} = \delta_{ij} G$  and Eq. (78) simplifies to,

$$G^{-1}_o(i\omega_r) = i\omega_r + \mu - G(i\omega_r)t^2 . \quad (80)$$

To evaluate Eq. (78) for a general density of states we write the one particle Green's function in terms of a self energy as in Eq. (16) and substitute Eq. (16) into the Fourier transform of Eq. (78). Using  $\int \frac{\rho(\epsilon)\epsilon^2}{Z-\epsilon} = Z \int \frac{\rho(\epsilon)\epsilon}{Z-\epsilon}$ ,  $t_{oo} = \sum_k t_k = \int \rho(\epsilon)\epsilon = 0$ , and  $\int \frac{\rho(\epsilon)}{Z-\epsilon}\epsilon = -1 + Z \int \frac{\rho(\epsilon)}{Z-\epsilon}$  to obtain the expression for  $G_o^{-1}$  in terms of  $G$  is,

$$G^{-1}_o(i\omega_r) = \frac{1}{G(i\omega_r)} - \Phi^{-1}(G(i\omega_r)) + \mu + i\omega_r, \quad (81)$$

$\Phi(Z) \equiv \int \frac{\rho(\epsilon)}{(Z-\epsilon)}$ .  $\Phi$  is the Hilbert transform of the lattice density of states and  $Z = i\omega_r + \mu - \Sigma(i\omega_r)$ .

---

## ACKNOWLEDGMENTS

The mean field theory for the strongly correlated problem was developed in collaboration with Dr. A. Georges. My own work on the Mott transition was carried out in collaboration with Marcelo Rozenberg, X. Y. Zhang, V. Dobrosavlevic, G. Moeller, and Q. Si. I am grateful to all of them for a most pleasant collaboration. I also acknowledge useful scientific exchanges with D. Fisher, A. Georges and W. Krauth. The financial support for this research was provided by the NSF under grant DMR 92-42000. The numerical part of this work was performed on a Cray Y/MP supercomputer of the NCSA in the University of Illinois at Urbana-Champaign.

---

## REFERENCES

1. D. Vollhardt in *Correlated Electron Systems*, ed. V. Emery (World Scientific, Singapore, 1993).
  2. W. Metzner and D. Vollhardt, *Phys. Rev. Lett.* **62**, 324 (1989).
  3. A. Georges and G. Kotliar, *Phys. Rev. B* **45**, 6479 (1992).
  4. U. Brandt and C. Mielsch, *Z. Phys.* **75**, 365 (1989); **79**, 295 (1990); **82**, 37(1991). V. Janis, *Z. Phys. B* **83**, 227 (1991).
  5. V. Janis and D. Vollhardt, *Int. Journ. Mod. Phys.* **B6**, 731 (1992).
  6. Q. Si and G. Kotliar, *Phys. Rev. Lett.* **70**, 3143 (1993).
  7. G. Kotliar and Q. Si, *Physica Scripta* **T49**, 165 (1993).
  8. For related work on impurity models by C. M. Varma and coworkers see C. M. Varma contribution to this volume and references therein.
  9. E. Müller-Hartmann, *Z. Phys. B* **74**, 507-512 (1989); *Z. Phys. B* **76**, 211-217 (1989).
  10. A. Georges, G. Kotliar and Q. Si, *Int. J. Mod. Phys.* **B6**, 705 (1992).
  11. A. Georges, G. Kotliar and W. Krauth, *Z. Fur Physik* in press.
  12. W. Krauth and M. Caffarel, preprint.
  13. A. Georges and W. Krauth, *Phys. Rev. Lett.* **69** (1992).
  14. X. Y. Zhang, M. J. Rozenberg and G. Kotliar, *Phys. Rev. Lett.* **70**, 1666 (1993).
  15. M. Jarrell, *Phys. Rev. Lett.* **69**, 168 (1992).
  16. Th. Pruschke, D. L. Cox and M. Jarrell, *Euro Phys. Letts.* **21**, 5 (1993), and *Phys. Rev. B* **47**, 3553 (1993).
-

17. A. Georges and W. Krauth, Phys. Rev. **B48**, 7167 (1993).
18. M. Rozenberg G. Kotliar, and X. Y.Zhang Phys. Rev. B (1994).
19. N. F. Mott, Phil. Mag. **6**, 287 (1961). N.F. Mott, Metal Insulator Trnastitions, Taylor and Francis LTD (1974).
20. J. Hubbard, Proc. Roy. Soc. (London) **A281**, 401 (1964).
21. W. F. Brinkman and T. M. Rice, Phys. Rev. B **2**, 4302 (1970).
22. J. C. Slater, Phys. Rev. **82**, 538 (1951).
23. M. J. Rozenberg, X. Y. Zhang, and G. Kotliar, Phys. Rev. Lett. **69**, 1236 (1992).
24. S. A. Carter, T. F. Rosenbaum, J. M. Honig, and J. Spalek, Phys. Rev. Lett. **67**, 3440 (1992).
25. Y. Tokura, Y. Taguchi, Y. Okada , Y. Fujishima, and T. Arima, K. Kumagai, Y. Iye, Phys. Rev. Letts. **70**, 2126 (1993).
26. J. Hirsch and R. Fye, Phys. Rev. Lett. **56**, 2521 (1986).
27. K. Yamada, Prog. Theor. Phys. **53**, 4 (1975) 970 K. Yosida and K. Yamada, *ibid.* 1286.
28. C. Castellani, G. Kotliar, R. Raimondi, M. Grilli, Z. Wang, and M. Rozenberg, Phys. Rev. Lett. **28**, 2009 (1992).
29. A. Fujimori, I. Hase, H. Namatame, Y. Fujishima, Y. Tokura, H. Eisaki, S. Uchida, K. Takegahara, and F. M. F. de Groot, Phys. Rev. Lett. **69**, 1796 (1992).
30. J. Freericks, Phys. Rev. **B41**, 9263 (1993).
31. Y. Tokura et al., Phys Rev Lett. **69**, 1796 (1992).
32. A. Chen, P. Yu, and D. Taylor Phys. Rev. Lett. **71**, 4011 (1993).
33. M. Pasternak et al., Phys. Rev. Lett. **65**, 790 (1990).
34. C. Castellani, C. Di Castro, D. Feinberg, and J. Raninger, Phys. Rev. Lett. **43**, 1957 (1979).
35. M. Rozenberg private communication.
36. G. Kotliar and A. Ruckenstein, Phys. Rev. Lett. **57**, 1362 (1986).
37. J. Spalek, A. Datta, and J. Honig, Phys. Rev. Lett. **54**, 728 (1987). For a review see J. Spalek, J. Sol. Stat. Chem. **88**, 70 (1990).
38. K. Honig and Appell, Phys. Rev. B **22**, 2626 (1980).
39. D. Vollhardt, Rev. Mod. Phys. **56**, 99 (1984).
40. M. Caffarel and W. Krauth preprint.
41. Q. Si M. Rozenberg G. Kotliar, and A. Ruckenstein, preprint.
42. M. Rozenberg G. Moeller, and G. Kotliar preprint.
43. V. Emery, Phys. Rev. Lett. **58**, 3759 (1987).
44. C. M. Varma, S. Shmitt Rink, and E. Abrahams, Solid State Comm. **62**, 681 (1987).
45. A. Georges and G. Kotliar, unpublished.
46. E. Gagliano et al., Phys. Rev. B **34**, (1986) 1677.
47. G. Moeller, Q. Si, G. Kotliar, and M. Rozenberg, preprint.
48. J. R. Schrieffer and P. A. Wolff, Phys. Rev. **149**, 491 (1966).
49. Q. Si, M. J. Rozenberg, G. Kotliar, and A. Ruckenstein, preprint (1993).

50. E. Dagotto and A. Moreo, Phys. Rev. D **31**, 865 (1985); E. Gagliano et al., Phys. Rev. B **34**, 1677 (1986).
51. V. Dobrosavlevic and G. Kotliar, Phys. Rev. Lett. **74**, 3218 (1993) and submitted to Phys. Rev. B.
52. V. Janis and D. Vollhardt, Phys. Rev. B **46**, 15712 (1992); V. Janis, M. Ulnke, and D. Vollhardt, Europhysics Lett. **24**, 287 (1993); G. S. Uhrig and R. Vlaming, preprint.
53. E. R. Gagliano and C. A. Balseiro, Phys. Rev. Lett. **59**, 2999 (1987).
54. B. Menge and E. Muller-Hartmann, Z. Phys. B **82**, 237 (1991).
55. H. Schweitzer and G. Czycholl, Z. Phys. B **83**, 93.

## DISCUSSION

**D. J. Scalapino:** Gabi, could you comment on the bipartite situation, and what the compressibility does as you change the filling towards half-filling. How does the compressibility vary? Do you see within your model how that changes?

**G. Kotliar:** That can be calculated. I have not investigated that. I don't think that there are any results on that yet. Let me explain what sort of difficulty [there is] in approaching the transition. It's only in the last six months that we finally have a method to get at the transition proper. The difficulty is, as I said, that there is a shrinking energy scale in the problem. So if you're solving the problem numerically — say you're doing quantum Monte Carlo — then you have  $U$ , which is two or three, and then you have this Kondo energy which is getting smaller and smaller and the numerics breaks down.

So we tried to look at this problem, to see whether the compressibility stayed finite, or went to zero, and with quantum Monte Carlo we couldn't resolve it. Now we have a new method that's more powerful — and that's the way that we were able to obtain the lifetimes and the relaxation time — which is based on renormalization group ideas. There we have really reduced the problem to an effective model, we get rid of the  $U$ , and then we have a problem with just one scale that we can crack numerically. And so far ... This is very recent; we've been doing that only for the last six months, and so far we've only used it at half filling. With that, probably, we will be able to answer your questions, so I think probably we'll know in two or three months.

**D. J. Scalapino:** The reason I think it's interesting is that ... I guess in one dimension, we know for the one-dimensional Hubbard model that the compressibility diverges as  $1/1-n$  ...

**G. Kotliar:** And Imada claims ...

**D. J. Scalapino:** ... And Imada claims, with Monte Carlo — up to, I guess,  $12 \times 12$  lattices — that in two dimensions, the variation of  $n$  versus  $\mu$  has this shape that would give rise to a similar result, and therefore I think it would be interesting to see what happens in  $d = \infty$ .

**G. Kotliar:** Yes, we tried, and actually we have Monte Carlo results which show  $dn/d\mu$  increases with decreasing temperature, but it does not seem to diverge. At zero temperature this question really cannot be answered with Monte Carlo — and I agree with you,  $d = \infty$  is interesting because we can take the thermodynamic limit — we really need to use some form of RG to nail the low energy, to answer that. But I completely agree with you. I think this is a very interesting question, which we are in a position to answer.

**H. Monien:** Yeah, I just wanted to know ... As far as I understand, you did all your calculations at half-filling, right? And ...

**G. Kotliar:** No, we have Monte Carlo runs away from half filling. For example, the  $\gamma$  as a function of doping was done away from half-filling.

**H. Monien:** I just wanted to know how you mapped out the pressure dependence in the experimental phase diagrams.

**G. Kotliar:** Oh, the pressure dependence in the experimental phase diagram ... Well, what we assume is that the pressure, what it does, is it changes the bandwidth. So the identification that you make is that as you change the pressure, you simply change the  $\frac{t}{U}$  of your Hubbard model. So, in this picture, this would be the temperature, and this would be  $1/U$ . So for small  $U$ , you have a metal, for large  $U$ , you have an insulator.

**J. W. Wilkins:** What is on the horizontal axis?

**G. Kotliar:** On the horizontal axis here is the increasing pressure, or internal pressure — that is, substitution by chromium or by titanium.

**J. W. Wilkins:** So it's concentration also?

**G. Kotliar:** Well, it is, if you do it like this.

**A. J. Millis:** I thought the philosophy was, you're not changing doping.

**G. Kotliar:** Unfortunately, the transition in this system occurs at negative pressure. But that's why I brought in the nickel iodide, which occurs at positive pressure, and I think this is a generic phase diagram of strongly correlated electron systems. You also see it in  $^3\text{He}$ , for example, if you're willing to buy that this is sort of a Hubbard model. And here, you can apply pressure, and temperature — you should think again of pressure as a bandwidth — and you see that you have a line of first-order transitions, and as you heat, you go from a liquid (which is like a metallic state) to the solid.

So I think that the phase diagram I present is sort of like a generic phase diagram with strong correlations, even though I cannot make a strong case that helium is a Hubbard model, or that  $\text{V}_2\text{O}_3$  is a Hubbard model. But I think that somehow the Hubbard model has some of the right physics of these systems. I think that one should look more carefully on the  $\text{NiI}_2$  system, because it has many advantages: simple band structure; the transition occurs at positive pressure; and again, it seems to be in the same class of materials.

**T. M. Rice:** I would like to ask if you could elaborate on the statement you are making that  $\text{V}_2\text{O}_3$  is not what you'd call a "Hubbard model."

**G. Kotliar:** Well, again, I'm sort of new to this subject, so I don't know very much. I asked the experts, and they referred me to two published things in the literature. One is ...

Okay, so first I looked at the band structure. Now, if you look at the band structure of  $V_2O_3$ , what you find is that the vanadium is a three-fold degenerate band; the degeneracy is lifted to something which is two-fold degenerate, and therefore you have two bands at the Fermi level. Then you look at the insulating side of  $V_2O_3$ , and then you find that the spin of the  $V_2O_3$  system is a spin one; not a spin one-half, but a spin one.

So then, you look at the literature to see why people thought of this in terms of Hubbard models, and then I found — you direct me to that reference — in Anderson's lectures in Varena, in which he somehow thinks that one should think in terms of the spin-one Hubbard model by looking at some molecular orbitals. The same view was expressed by Varma in his Les Houches lectures. The only real calculation I know of is a calculation by Castellani et al., but again, I don't know of any mapping of the  $V_2O_3$  on a one-band Hubbard model; I think it's not possible. But I think that somehow Hubbard physics is the right physics; one has to think more carefully about the quantum chemistry of that problem.

And again, I want to stress that the phase diagram occurs not just for  $V_2O_3$ ; it occurs for helium, it occurs for  $NiI_2$ . So I think that there's something right about these ideas as sort of generic ideas for understanding phase diagrams of strongly correlated electron systems.

**C. M. Varma:** Gabi, my question concerns your results on the enhancement of the resistivity and the nuclear relaxation rate. My point is that in front of nuclear relaxation rate — not  $\chi''$  — there is also a matrix element of the hyperfine interaction squared, which has wavefunction renormalization (same thing as vertex renormalizations), and those wavefunction renormalizations exactly cancel ...

**G. Kotliar:** Okay, then I may have been too fast in connecting that with  $1/T_1T$ . The thing that we did calculate is simply this quantity:  $\sum_q \frac{\chi''(q, \omega)}{\omega}$ . Okay?

**C. M. Varma:** Okay, I see what you mean.

**G. Kotliar:** And we have not put the matrix elements yet.

**C. M. Varma:** Okay. But is the method in principle capable of calculating vertex corrections?

**G. Kotliar:** Yeah, of course, all the vertex corrections in quantities which have *s*-wave symmetry — like susceptibility, compressibility — are there; there are no vertex corrections in things like conductivities.

**J. W. Wilkins:** Well, I was sitting reading my e-mail this morning, innocently, and in came this question: "Does anyone know anything about the phase diagram of the Hubbard model, particularly as the system is doped away from half-filling." And of course at first, when I heard your talk, I thought you were always at half-filling, but then I started seeing things that were away from half-filling. So they would be fascinated to know about the nature of the metal-insulator transition, as the doping changes. And since you've got a piece of paper there, perhaps you could sketch the phase diagram, and then all these colleagues could correct it for you.

**G. Kotliar:** No, John, I think that this is basically on the same vein as the question of Doug Scalapino. At this point, I don't think I want to make any statements as to what's happening to the Hubbard model away from half-filling, as far as a very precise phase diagram. I can guess for you, but I don't know of any realistic calculations. So let me give you my guesses, but they're only that: guesses. We haven't done any work on that, and I'm not aware of any published work in the literature.

So we start with a Néel state (if you are in a bipartite lattice). So what is the problem? Well, presumably the Néel temperature will go down as a function of doping. This is very hard to calculate, because presumably there is some incommensurate order going in here. These are the things which are not captured very well in large dimensions. So this curve would be very interesting to get; I don't think anybody has gotten it.

Now, if you are in the fully frustrated case, so we have, at half-filling, when  $\delta = 0$ , we have these two critical values of  $U$ :  $U_{c1}$  and  $U_{c2}$ . Then you would like to know what happens when I move along this axis. Well, my guess is that, since at zero temperature now we know that the metal is always stable, the phase diagram here is always a Fermi liquid. But again, I would like to see some numerical demonstration of that. And I stress the problem is that approaching these points here [ $U_{c1}$  and  $U_{c2}$ ], you run into the problem of having small energy scales, and therefore you need clever numerical methods like the RG that you and your collaborators developed several years ago, or the things that we are doing now which are just simple modifications of that to apply to infinite dimensions, to try to answer this class of questions.

**D. Schmeltzer:** My question is on the first part, on the conceptual level, actually: how the Luttinger theorem occurs here, since the number of particles always goes to infinity, here you have to have, to keep it fixed. And then the other point is that in any dimension where you are, if you have a Fermi surface there is an order parameter, and the quantum fluctuations are always of one-dimensional nature, at least for the particle-hole part.

**G. Kotliar:** Yeah.

**D. Schmeltzer:** So how does this come in ...

**G. Kotliar:** How the Luttinger theorem works is very simple.  $G(\omega, k)$ , as Chandra just mentioned, is given by  $\frac{1}{\omega - \epsilon_k - \sum(\omega) + \mu}$ , and you can show that if you evaluate  $\sum$  exactly for small  $U$ , then the volume of the Fermi surface doesn't change. And the manifestation of that is that the imaginary part of  $\sum(\omega)$  goes to zero, which simply implies that the integral of  $G(\omega, k)$ , which is  $G(0)$  [ $\sum_k G(\omega, k) = G(0)$ ], is simply unrenormalized. So Luttinger theorem is obeyed, in this limit of large dimensions for small values of  $U$ ; it's not obeyed for large values of  $U$  because you have a Mott transition.

So, coming to the second part of the question about the one-dimensional nature of the fluctuations: What we're doing here is somewhat different from the bosonization scheme that you're thinking about. Here what we're doing, conceptually, is we're taking the quantum mechanics on the imaginary axis exactly, and we're sort of butchering the spatial parts, and reducing the problem to a single-site problem. It's very different, conceptually, from the bosonization treatment, which tries to think of the Fermi surface [as] sort of a one-dimensional object with many directions. And, in particular, it may be that this mean-field theory does very poorly in two dimensions. But, I think that I convinced you that we're doing something right, at least for three dimensions.

**G. T. Zimanyi:** Speaking of frustrated Hubbard models, there is an interesting paper of Krishnamurthi, Jayaprakash, and coworkers on the Hubbard model for the triangular lattice, that they show that even at half-filling, you can have magnetic ordering with a  $q$  vector different from simple commensurate values. So my first question is: Can your technique pick up such incommensurate orderings, even at half-filling.

And secondly, just as a vague remark, that you showed the vanadium oxide phase diagram of Rosenbaum et al. which also shows an incommensurate ordering, and at least it's interesting to speculate that maybe these two types of incommensurate orderings could be related, further enhancing the notion that vanadium oxide, after all, is described by Hubbard model ...

**G. Kotliar:** I agree with you. I think that, in principle, it can be done. I mean, the crucial observation in this respect was actually made by Jim Freericks, who noticed that for a long time people claimed that in infinite  $d$  you couldn't detect incommensurate order. But what Jim Freericks noticed is that you can calculate some susceptibility  $\chi(q)$ , and it depends on a variable  $\sum_{\alpha=1}^d \cos k_{\alpha}$ ; let's call that "x." So then you can look at this  $\chi$  as a function of this variable  $x$ , and see where it becomes unstable. And then, depending on the structure, it could become unstable, and he demonstrated it becomes unstable in sort of a Falicov-Kimball model, at incommensurate values.

We have not investigated that. The reason why we studied so thoroughly the half-full Hubbard model is because we needed to develop the tools and the machinery to crack this class of functional equations in sort of a somewhat simple context. But we have not tried to address any of the more complicated questions; we really moved in different directions.

Now, you want to ask about the phase diagram of  $V_2O_3$ , right Gabe?

**G. Aeppli:** I just wanted to point out that the incommensurate order in the metal has nothing to do with the commensurate order in pure  $V_2O_3$ .

**G. Kotliar:** Yeah, and I think that's exactly what the large  $d$  would predict, because the phase diagram that you have in that case has this line of first-order phase transitions, and here [pointing to left side of diagram], if you are in an arbitrary lattice, I think you have something like ... there are really two solutions, which have nothing to do with each other.